UNIVERSIDAD DE CONCEPCIÓN

Centro de Investigación en Ingeniería Matemática (CI²MA)

Conservative discontinuous finite volume and mixed schemes for a new four-field formulation in poroelasticity

Sarvesh Kumar, Ricardo Oyarzúa,
Ricardo Ruiz-Baier, Ruchi Sandilya

PREPRINT 2018-32

SERIE DE PRE-PUBLICACIONES

Conservative discontinuous finite volume and mixed schemes for a new four-field formulation in poroelasticity *

Sarvesh Kumar† Ricardo Oyarzúa‡ Ricardo Ruiz-Baier§ Ruchi Sandilya¶

July 4, 2018

Abstract

We introduce a hybrid numerical method for the approximation of linear poroelasticity equations, representing the interaction between the non-viscous filtration flow of a fluid and the linear mechanical response of a porous medium. In the proposed formulation, the primary variables in the system are the solid displacement, the fluid pressure, the fluid flux, and the total pressure. A discontinuous finite volume method is designed for the approximation of solid displacement using a dual mesh, whereas a mixed approach is employed to approximate fluid flux and the two pressures. The resulting discrete problems exhibit a double saddle-point structure, and their solvability and stability are established in terms of bounds that do not depend on the modulus of dilation of the solid. We derive optimal error estimates in suitable norms, for all field variables; and we exemplify the convergence and locking-free properties of this scheme through a series of numerical tests.

Key words: Biot consolidation problem; Discontinuous finite volume methods; Mixed finite elements; Locking-free approximations; Conservative schemes; Error estimates.

Mathematics subject classifications (2010): 65N30; 76S05; 74F10; 65N15.

1 Introduction

The linear poroelasticity equations constitute one of the simplest continuum models for fluid-structure interaction. In the classical description of the consolidation problem by Biot (see the seminal paper [5]), the filtration of a viscous fluid within the porous skeleton is described by Darcy's law, whereas the deformation of the solid material is governed by Hooke's linear elasticity. Modern applications of this classical framework include numerous problems in science and engineering, where notable examples are logging technologies and the study of borehole instabilities, the behaviour of soils under tunnelling, or in the process of CO_2 sequestration; as well as biomedical investigations such as the characterisation of biological soft tissue (e.g. arterial walls, skin, lungs, cardiac muscle, and articular cartilage).

*This research was partially supported by CONICYT-Chile through project Fondecyt 1161325 and project AFB170001 of the PIA Program: Concurso Apoyo a Centros Cientificos y Tecnologicos de Excelencia con Financiamiento Basal.

†Department of Mathematics, Indian Institute of Space Science and Technology, Thiruvananthapuram 695 547, Kerala, India. E-mail: sarvesh@iist.ac.in.

‡GIMNAP, Departamento de Matemática, Universidad del Bío-Bío, Casilla 5-C, Concepción, Chile; and Centro de Investigación en Ingeniería Matemática (CI^{2}MA), Universidad de Concepción, Chile. E-mail: royarzua@ubiobio.cl.

§Mathematical Institute, Oxford University, Andrew Wiles Building, Woodstock Road, OX2 6GG Oxford, UK. E-mail: ruizbaier@maths.ox.ac.uk.

¶Tata Institute of Fundamental Research, Centre for Applicable Mathematics, Bangalore 560065, India. E-mail: ruchi@tifrbng.res.in

Due to the coupling of flow, transport, and conservation of linear momentum, obtaining analytical solutions for poroelasticity equations is not trivial. One therefore has to rely on computational simulations. However, the success in accurately replicating poroelasticity solutions using numerical methods is often affected by the presence of three unphysical scenarios: spurious pressure modes, locking phenomena (instabilities and polluted convergence of the solid displacement approximation), and loss of mass. In view of remediating these shortcomings encountered in the solutions produced with classical methods and formulations, here we extend the three-field formulation proposed in [19, 25] (where classical finite elements can be employed straightforwardly without the risk of producing the first two spurious phenomena), and we further introduce a family of discontinuous finite volume (DFV) - mixed finite element (MFE) schemes that aim at rectifying the third nonphysical situation.

With the exception of the finite volume (FV) discretisation of Biot's system applied in [3, 23], the numerical solution of poroelasticity equations has been traditionally associated with finite element (FE) methods. Some of these studies include stabilised conforming schemes for primal formulations and least-squares FE methods [1, 4, 12, 21, 22, 31, 32, 35] (see also the extensive review [20]); as well as DG methods [9, 28]. On the other hand, a few schemes that combine discontinuous Galerkin (or finite volume, or weak Galerkin) discretisations and mixed methods solving also for the fluid flux, have been proposed in [26, 29, 30, 34]. Apart from reproducing accurately the mechanical equilibrium, guaranteeing the conservation of fluid mass is of substantial importance in most applications. Some dedicated techniques are available, including for instance the stabilised method in [10]; and the reconstruction of stress and fluid fluxes by a modified Arnold-Winther scheme, recently analysed in [27].

Here we also aim at developing stable and convergent schemes using similar techniques; but the primary differences with respect to the contributions listed above is that we use a special blend of DFV and MFE methods for the numerical approximation of the underlying coupled problem, recast in terms of solid displacement, fluid flux, fluid pressure, and total pressure. FV schemes are a particular class of Petrov-Galerkin methods that require to define trial and test spaces associated to primal and dual partitions of the domain, respectively. Different types of dual meshes are employed when the FV method is of conforming, non-nonconforming, or discontinuous type (see details and comparisons in e.g. [8]), but in most cases they feature local conservativity as well as suitability for deriving L^2-error estimates. Moreover, schemes using DFV approximations preserve features of both DG and general FV methods, including smaller support of dual elements (when compared with conforming and non-conforming FV schemes) as well as appropriateness in handling discontinuous coefficients.

We have structured the contents of this paper as follows. Section 2 outlines the main ingredients of the model problem and carry out its solvability and stability analysis. A family of DFV-MFE methods is then introduced in Section 3, and the invertibility of the discrete solution operator is derived in Section 4. The error analysis of the proposed schemes is addressed next in Section 5, and in Section 6 we provide a few numerical tests illustrating the properties of the proposed method.

2 The governing equations in a mixed-mixed structure

Preliminaries. From now on we will adopt the classical notation for Lebesgue and Sobolev spaces. In addition by $\mathbf{M}$ and $\mathbb{M}$ we will denote the corresponding vectorial and tensorial counterparts of the generic scalar functional space M. For instance, if $\Theta \subseteq \mathrm{R}^d$, $d = 2, 3$ is a domain, $\Lambda \subseteq \mathrm{R}^d$ is a Lipschitz surface, and $r \in \mathrm{R}$, we define $\mathbf{H}^r(\Theta) := [\mathrm{H}^r(\Theta)]^d$ and $\mathbf{H}^r(\Lambda) := [\mathrm{H}^r(\Lambda)]^d$. By $\mathbf{0}$ we will refer to the generic zero vector and we will denote by C and c, with or without subscripts, bars, tildes or hats, generic constants independent of the discretisation parameters. We recall that $\mathbf{H}(\mathrm{div};\Theta) := \{\boldsymbol{\tau} \in \mathbf{L}^2(\Theta) : \nabla \cdot \boldsymbol{\tau} \in L^2(\Theta)\}$ associated with the norm

$$\|\boldsymbol{\tau}\|^2_{\mathrm{div},\Theta} := \|\boldsymbol{\tau}\|^2_{0,\Theta} + \|\nabla \cdot \boldsymbol{\tau}\|^2_{0,\Theta}\,,$$

is a Hilbert space.

As a model problem we consider a homogeneous porous medium constituted by a mixture of incompressible grains and interstitial fluid. The domain of interest $\Omega \subset \mathrm{R}^d$, $d = 2, 3$ is assumed bounded and simply connected. For a given body force $\boldsymbol{f}$ and a given volumetric fluid source ℓ, we will concentrate the discussion on the following four-field mixed-mixed formulation of Biot's consolidation system: find the displacements of the porous skeleton, $\boldsymbol{u}$, the total pore pressure of the fluid, p, the fluid flux, $\boldsymbol{\sigma}$, and the total fluid-structure pressure (or total volumetric stress), ϕ; satisfying

$$-\mathbf{div}(2\mu\boldsymbol{\varepsilon}(\boldsymbol{u}) - \phi\mathbf{I}) = \boldsymbol{f} \qquad \text{in } \Omega, \tag{2.1}$$

$$\phi = p - \lambda \operatorname{div} \boldsymbol{u} \qquad \text{in } \Omega, \tag{2.2}$$

$$\boldsymbol{\sigma} = -\frac{\kappa}{\eta}(\nabla p - \rho \boldsymbol{g}) \qquad \text{in } \Omega, \tag{2.3}$$

$$\left(c_0 + \frac{\alpha}{\lambda}\right) p - \frac{\alpha}{\lambda}\phi + \operatorname{div} \boldsymbol{\sigma} = \ell \qquad \text{in } \Omega, \tag{2.4}$$

where $\boldsymbol{\varepsilon}(\boldsymbol{u}) = \frac{1}{2}(\nabla \boldsymbol{u} + \nabla \boldsymbol{u}^T)$ is the tensor of infinitesimal strains, κ is the permeability of the porous solid (assumed uniformly bounded $0 < \kappa_1 \leq \kappa(\boldsymbol{x}) \leq \kappa_2 < \infty$, for all $\boldsymbol{x} \in \Omega$), λ, μ are the Lamé constants of the solid (moduli of dilation and shear, respectively), $c_0 > 0$ is the constrained specific storage coefficient, $\alpha > 0$ is the Biot-Willis parameter, $\boldsymbol{g}$ is the gravity acceleration; and $\eta > 0, \rho > 0$ are the viscosity and density of the pore fluid. Equation (2.1) states conservation of momentum for the mixture, (2.4) corresponds to the mass conservation of the fluid content, and (2.2)-(2.3) define the new unknowns in the system in terms of the primal variables.

The boundary of Ω is assumed disjointly split into segments or surfaces where Dirichlet conditions are to be considered for fluid pressure and solid displacements: $\partial\Omega = \overline{\Gamma}_p \cup \overline{\Gamma}_{\boldsymbol{u}}$, $\Gamma_p \cap \Gamma_{\boldsymbol{u}} = \emptyset$. These prescriptions are accompanied by zero normal total stress, and by zero normal fluid flux, respectively. In summary, we endow the system (2.1)-(2.4) with the following boundary conditions

$$p = p_\Gamma, \ (2\mu\boldsymbol{\varepsilon}(\boldsymbol{u}) - \phi\mathbf{I})\,\boldsymbol{n} = \mathbf{0} \text{ on } \Gamma_p, \quad \text{and} \quad \boldsymbol{u} = \mathbf{0}, \ \boldsymbol{\sigma}\cdot\boldsymbol{n} = 0 \text{ on } \Gamma_{\boldsymbol{u}}, \tag{2.5}$$

where $\boldsymbol{n}$ is the exterior unit normal vector on $\partial\Omega$ and $p_\Gamma \in \mathrm{H}^{1/2}_{00}(\Gamma_p) := \{v|_{\Gamma_p} \,:\, v \in \mathrm{H}^1_{\Gamma_{\boldsymbol{u}}}(\Omega)\}$, with $\mathrm{H}^1_{\Gamma_{\boldsymbol{u}}}(\Omega) := \{v \in \mathrm{H}^1(\Omega) \,:\, v|_{\Gamma_{\boldsymbol{u}}} = 0\}$. The space $\mathrm{H}^{1/2}_{00}(\Gamma_p)$ is endowed with the norm

$$\|\xi\|_{1/2,00,\Gamma_p} := \inf\{\|v\|_{1,\Omega} : v \in \mathrm{H}^1_{\Gamma_{\boldsymbol{u}}}(\Omega) \quad \text{and} \quad v|_{\Gamma_p} = \xi\}.$$

Weak formulation. We proceed to test equations (2.1)-(2.4) against appropriate functions and to integrate by parts. This step leads to the following weak formulation of the coupled problem: find $\boldsymbol{u} \in \mathbf{H}$, $\phi \in \mathrm{Q}$, $\boldsymbol{\sigma} \in \mathbf{Z}$, and $p \in \mathrm{Q}$ such that

$$a_s(\boldsymbol{u}, \boldsymbol{v}) + b_s(\boldsymbol{v}, \phi) = F(\boldsymbol{v}) \quad \forall \boldsymbol{v} \in \mathbf{H}, \tag{2.6}$$

$$b_s(\boldsymbol{u}, \psi) - c_s(\phi, \psi) + b_{sf}(\psi, p) = 0 \quad \forall \psi \in \mathrm{Q}, \tag{2.7}$$

$$a_f(\boldsymbol{\sigma}, \boldsymbol{\tau}) + b_f(\boldsymbol{\tau}, p) = G(\boldsymbol{\tau}) \quad \forall \boldsymbol{\tau} \in \mathbf{Z}, \tag{2.8}$$

$$b_{sf}(\phi, q) + b_f(\boldsymbol{\sigma}, q) - c_f(p, q) = H(q) \quad \forall q \in \mathrm{Q}, \tag{2.9}$$

where the bilinear forms and linear functionals appearing in (2.6)–(2.9) (denoted with a subscript s or f whenever the arguments are solely related to structure or to fluid variables, respectively) are specified in the following way

$$\begin{aligned} &a_s(\boldsymbol{u}, \boldsymbol{v}) := 2\mu\int_\Omega \boldsymbol{\varepsilon}(\boldsymbol{u}) : \boldsymbol{\varepsilon}(\boldsymbol{v}), \quad b_s(\boldsymbol{v}, \psi) := -\int_\Omega \psi \operatorname{div} \boldsymbol{v}, \quad b_{sf}(\psi, q) := \frac{1}{\lambda}\int_\Omega \psi q, \ c_s(\phi, \psi) := \frac{1}{\lambda}\int_\Omega \phi\psi, \\ &a_f(\boldsymbol{\sigma}, \boldsymbol{\tau}) := \frac{\eta}{\kappa\alpha}\int_\Omega \boldsymbol{\sigma}\cdot\boldsymbol{\tau}, \quad b_f(\boldsymbol{\tau}, q) := -\frac{1}{\alpha}\int_\Omega q \operatorname{div} \boldsymbol{\tau}, \quad c_f(p, q) := \left(\frac{c_0}{\alpha} + \frac{1}{\lambda}\right)\int_\Omega pq, \\ &F(\boldsymbol{v}) := \int_\Omega \boldsymbol{f}\cdot\boldsymbol{v}, \quad G(\boldsymbol{\tau}) := \frac{1}{\alpha}\int_\Omega \rho\boldsymbol{g}\cdot\boldsymbol{\tau} - \frac{1}{\alpha}\langle\boldsymbol{\tau}\cdot\boldsymbol{n}, p_\Gamma\rangle_{\Gamma_p}, \quad H(q) := -\frac{1}{\alpha}\int_\Omega \ell\, q, \end{aligned} \tag{2.10}$$

and the conditions in (2.5) imply that the functional spaces may be chosen as

$$\mathbf{H} := \mathbf{H}^1_{\Gamma_{\boldsymbol{u}}}(\Omega) = \{\boldsymbol{v} \in \mathbf{H}^1(\Omega) : \boldsymbol{v}|_{\Gamma_{\boldsymbol{u}}} = \mathbf{0}\},\ \mathrm{Q} := \mathrm{L}^2(\Omega),\ \mathbf{Z} := \{\boldsymbol{\tau} \in \mathbf{H}(\mathrm{div};\Omega) : \boldsymbol{\tau}\cdot\boldsymbol{n} = 0 \text{ on } \Gamma_{\boldsymbol{u}}\}.$$

Notice that the mixed character of the fluid conservation equation implies that the Dirichlet datum for the fluid pressure appears in the linear functional G.

Properties of the involved forms. Thanks to the Cauchy-Schwarz inequality, it is readily seen that all bilinear forms and linear functionals are uniformly bounded, that is

$$\begin{aligned}
&|a_s(\boldsymbol{u},\boldsymbol{v})| \le 2\mu C_{k,2}\|\boldsymbol{u}\|_{1,\Omega}\|\boldsymbol{v}\|_{1,\Omega}, \quad |a_f(\boldsymbol{\sigma},\boldsymbol{\tau})| \le \frac{\eta}{\alpha\kappa_1}\|\boldsymbol{\sigma}\|_{\mathrm{div},\Omega}\|\boldsymbol{\tau}\|_{\mathrm{div},\Omega},\\
&|b_s(\boldsymbol{v},\psi)| \le \|\boldsymbol{v}\|_{1,\Omega}\|\psi\|_{0,\Omega}, \quad |b_{sf}(\psi,q)| \le \lambda^{-1}\|\psi\|_{0,\Omega}\|q\|_{0,\Omega}, \quad |b_f(\boldsymbol{\tau},q)| \le \|\boldsymbol{\tau}\|_{\mathrm{div},\Omega}\|q\|_{0,\Omega},\\
&|c_s(\phi,\psi)| \le \lambda^{-1}\|\phi\|_{0,\Omega}\|\psi\|_{0,\Omega}, \quad |c_f(p,q)| \le \big(\frac{c_0}{\alpha}+\frac{1}{\lambda}\big)\|p\|_{0,\Omega}\|q\|_{0,\Omega},
\end{aligned} \tag{2.11}$$

and

$$|F(\boldsymbol{v})| \le \|\boldsymbol{f}\|_{0,\Omega}\|\boldsymbol{v}\|_{1,\Omega},\ |G(\boldsymbol{\tau})| \le \frac{1}{\alpha}(\rho\|\boldsymbol{g}\|_{0,\Omega} + \|p_\Gamma\|_{1/2,00,\Gamma_p})\|\boldsymbol{\tau}\|_{\mathrm{div},\Omega},\ |H(q)| \le \frac{1}{\alpha}\|\ell\|_{0,\Omega}\|q\|_{0,\Omega}, \tag{2.12}$$

for all $\boldsymbol{u},\boldsymbol{v} \in \mathbf{H}$, $p,q,\phi,\psi \in \mathrm{Q}$, $\boldsymbol{\sigma},\boldsymbol{\tau} \in \mathbf{Z}$. Above, $C_{k,2}$ is one of the positive constants satisfying

$$C_{k,1}\|\boldsymbol{v}\|^2_{1,\Omega} \le \|\boldsymbol{\varepsilon}(\boldsymbol{v})\|^2_{0,\Omega} \le C_{k,2}\|\boldsymbol{v}\|^2_{1,\Omega}, \quad \forall\, \boldsymbol{v} \in \mathbf{H}. \tag{2.13}$$

Regarding the positivity of the forms a_s and a_f, we begin by using (2.13), to obtain

$$a_s(\boldsymbol{v},\boldsymbol{v}) \ge 2\mu C_{k,1}\|\boldsymbol{v}\|^2_{1,\Omega}, \quad \forall\, \boldsymbol{v} \in \mathbf{H}. \tag{2.14}$$

In turn, we define

$$K_f := \{\boldsymbol{\tau} \in \mathbf{Z} : b_f(\boldsymbol{\tau},q) = 0 \quad \forall\, q \in \mathrm{Q}\} = \{\boldsymbol{\tau} \in \mathbf{Z} : \mathrm{div}\,\boldsymbol{\tau} = 0 \quad \text{in} \quad \Omega\},$$

and observe that the following inequality holds

$$a_f(\boldsymbol{\tau},\boldsymbol{\tau}) \ge \frac{\eta}{\kappa_2\alpha}\|\boldsymbol{\tau}\|^2_{\mathrm{div},\Omega}, \quad \forall\, \boldsymbol{\tau} \in \mathbf{Z}. \tag{2.15}$$

Finally, we recall the following inf-sup conditions satisfied by the forms b_s and b_f (see e.g. [15]):

$$\sup_{\boldsymbol{v}\in\mathbf{H}\setminus\mathbf{0}} \frac{b_s(\boldsymbol{v},\psi)}{\|\boldsymbol{v}\|_{1,\Omega}} \ge \beta_s\|\psi\|_{0,\Omega} \quad \forall\, \psi \in \mathrm{Q} \quad \text{and} \quad \sup_{\boldsymbol{\tau}\in\mathbf{Z}\setminus\mathbf{0}} \frac{b_f(\boldsymbol{\tau},q)}{\|\boldsymbol{\tau}\|_{\mathrm{div},\Omega}} \ge \alpha^{-1}\beta_f\|q\|_{0,\Omega} \quad \forall\, q \in \mathrm{Q}, \tag{2.16}$$

with $\beta_s,\beta_f > 0$ depending on $|\Omega|$.

Analysis of the continuous problem. In what follows we establish the well-posedness and stability of our formulation. To that end we derive the continuous dependence result for (2.6)–(2.9) by considering generic functionals at the corresponding right-hand side. Then, recalling that the problem is symmetric, the existence, uniqueness and stability of solution can be easily obtained from the aforementioned result. In addition, we observe in advance that the discrete version of the following theorem, whose proof can be obtained by following the same steps provided next, is crucial for the derivation of the corresponding error estimate. Let us then define $F_1 \in \mathbf{H}'$, $G_1 \in \mathrm{Q}'$, $F_2 \in \mathbf{Z}'$ and $G_2 \in \mathrm{Q}'$ and let $(\boldsymbol{u},\phi,\boldsymbol{\sigma},p) \in \mathbf{H}\times\mathrm{Q}\times\mathbf{Z}\times\mathrm{Q}$, be such that

$$a_s(\boldsymbol{u},\boldsymbol{v}) + b_s(\boldsymbol{v},\phi) = F_1(\boldsymbol{v}) \quad \forall \boldsymbol{v} \in \mathbf{H}, \tag{2.17}$$

$$b_s(\boldsymbol{u},\psi) - c_s(\phi,\psi) + b_{sf}(\psi,p) = G_1(\psi) \quad \forall \psi \in \mathrm{Q}, \tag{2.18}$$

$$a_f(\boldsymbol{\sigma},\boldsymbol{\tau}) + b_f(\boldsymbol{\tau},p) = F_2(\boldsymbol{\tau}) \quad \forall \boldsymbol{\tau} \in \mathbf{Z}, \tag{2.19}$$

$$b_{sf}(\phi,q) + b_f(\boldsymbol{\sigma},q) - c_f(p,q) = G_2(q) \quad \forall q \in \mathrm{Q}. \tag{2.20}$$

For the subsequent analysis we will appeal to preliminary results and definitions. We begin by observing that each $\boldsymbol{\tau}$ in $\mathbf{Z}$ can be uniquely decomposed into the form

$$\boldsymbol{\tau} = \boldsymbol{\tau}_0 + \boldsymbol{\tau}^{\perp}, \text{ with } \boldsymbol{\tau}_0 \in K_f \text{ and } \boldsymbol{\tau}^{\perp} \in K_f^{\perp}.$$

Then, we define $F_2^0 \in K_f'$ and $F_2^{\perp} \in (K_f^{\perp})'$ be such that

$$F_2(\boldsymbol{\tau}) = F_2^0(\boldsymbol{\tau}_0) + F_2^{\perp}(\boldsymbol{\tau}^{\perp}) \quad \forall\, \boldsymbol{\tau} = \boldsymbol{\tau}_0 + \boldsymbol{\tau}^{\perp} \in \mathbf{Z}. \tag{2.21}$$

Clearly

$$F_2|_{K_f}(\boldsymbol{\tau}) = F_2^0(\boldsymbol{\tau}_0), \quad F_2|_{K_f^{\perp}}(\boldsymbol{\tau}) = F_2^{\perp}(\boldsymbol{\tau}^{\perp}), \quad F_2^0(\boldsymbol{\tau}^{\perp}) = 0 \quad \text{and} \quad F_2^{\perp}(\boldsymbol{\tau}_0) = 0. \tag{2.22}$$

Similarly, we define

$$K_s := \{\boldsymbol{v} \in \mathbf{H} : b_s(\boldsymbol{v},\psi) = 0 \quad \forall\, \psi \in \mathrm{Q}\},$$

and observe that each $\boldsymbol{v}$ in $\mathbf{H}$ can be uniquely decomposed into the form

$$\boldsymbol{v} = \boldsymbol{v}_0 + \boldsymbol{v}^{\perp}, \text{ with } \boldsymbol{v}_0 \in K_s \text{ and } \boldsymbol{v}^{\perp} \in K_s^{\perp}.$$

Let us now observe that from the inf-sup conditions (2.16), there holds

$$\sup_{(\boldsymbol{v},\boldsymbol{\tau})\in(\mathbf{H}\times\mathbf{Z})\setminus\mathbf{0}} \frac{b_s(\boldsymbol{v},\psi) + b_f(\boldsymbol{\tau},q)}{\|\boldsymbol{v}\|_{1,\Omega} + \|\boldsymbol{\tau}\|_{\mathrm{div},\Omega}} \geq \beta(\|\psi\|_{0,\Omega} + \|q\|_{0,\Omega}) \quad \forall\, \psi, q \in \mathrm{Q}, \tag{2.23}$$

with $\beta > 0$ independent of λ. From (2.23) and [13, Lemma 2.1] it can be easily deduced that

$$\sup_{(\psi,q)\in(\mathrm{Q}\times\mathrm{Q})\setminus\mathbf{0}} \frac{b_s(\boldsymbol{v}^{\perp},\psi) + b_f(\boldsymbol{\tau}^{\perp},q)}{\|\psi\|_{0,\Omega} + \|q\|_{0,\Omega}} \geq \beta(\|\boldsymbol{v}^{\perp}\|_{1,\Omega} + \|\boldsymbol{\tau}^{\perp}\|_{\mathrm{div},\Omega}) \quad \forall\, (\boldsymbol{v}^{\perp},\boldsymbol{\tau}^{\perp}) \in K_s^{\perp} \times K_f^{\perp}. \tag{2.24}$$

To conclude we define

$$\begin{aligned} C((\phi,p),(\psi,q)) :=& \quad c_s(\phi,\psi) + c_f(p,q) - b_{sf}(\phi,q) - b_{sf}(\psi,p) \\ =& \quad \frac{1}{\lambda}\int_{\Omega}(\phi - p)(\psi - q) + \frac{c_0}{\alpha}\int_{\Omega} pq, \quad \forall\, \phi,\psi,p,q \in \mathrm{Q}, \end{aligned}$$

and notice that

$$\begin{aligned} |C((\phi,p),(\psi,q))| \leq& \quad C((\phi,p),(\phi,p)))^{1/2}(C((\psi,q),(\psi,q)))^{1/2} \\ =& \quad \left(\frac{1}{\lambda}\|\phi - p\|_{0,\Omega}^2 + \frac{c_0}{\alpha}\|p\|_{0,\Omega}^2\right)^{1/2}\left(\frac{1}{\lambda}\|\psi - q\|_{0,\Omega}^2 + \frac{c_0}{\alpha}\|q\|_{0,\Omega}^2\right)^{1/2}, \end{aligned} \tag{2.25}$$

for all $\phi,\psi,p,q \in \mathrm{Q}$, and

$$C((\psi,q),(\psi,q)) = \frac{1}{\lambda}\|\psi - q\|_{0,\Omega}^2 + \frac{c_0}{\alpha}\|q\|_{0,\Omega}^2 \geq \frac{c_0}{\alpha}\|q\|_{0,\Omega}^2. \tag{2.26}$$

Theorem 2.1 *Let $(\boldsymbol{u},\phi,\boldsymbol{\sigma},p) \in \mathbf{H}\times\mathrm{Q}\times\mathbf{Z}\times\mathrm{Q}$ be such that the system (2.17)–(2.20) holds. Then, there exists a constant $C > 0$, independent of λ, such that*

$$\|\boldsymbol{u}\|_{1,\Omega} + \|\phi\|_{0,\Omega} + \|\boldsymbol{\sigma}\|_{\mathrm{div},\Omega} + \|p\|_{0,\Omega} \leq C(\|F_1\|_{\mathbf{H}'} + \|G_1\|_{\mathrm{Q}'} + \|F_2\|_{\mathbf{Z}'} + \|G_2\|_{\mathrm{Q}'}).$$

Proof. Proceeding similarly to the proof of [6, Theorem 4.3.1], we will perform three steps. Firstly, we assume that $G_1 = 0$ and $F_2 = 0$ and bound the solution in terms of F_1 and G_2. Secondly, we assume that $F_1 = 0$, $G_2 = 0$, $G_1 = 0$ and derive an estimate for the solution in terms of F_2. Finally, we assume that $F_1 = 0$, $G_2 = 0$ and $F_2 = 0$ and derive an estimate for the solution in terms of G_1. In this way, the desired stability will follow by linearity after adding the obtained estimates.

Step 1 ($G_1 = 0$ and $F_2 = 0$): Taking $\boldsymbol{v} = \boldsymbol{u}$ in (2.17), $\psi = \phi$ in (2.18), $\boldsymbol{\tau} = \boldsymbol{\sigma}$ in (2.8) and $q = p$ in (2.20) and performing the operations (2.17) − (2.18) + (2.19) − (2.20), we obtain

$$a_s(\boldsymbol{u}, \boldsymbol{u}) + a_f(\boldsymbol{\sigma}, \boldsymbol{\sigma}) + C((\phi, p), (\phi, p)) = F_1(\boldsymbol{u}) + G_2(p).$$

Then, applying (2.14),(2.26) and the boundedness of F_1 and G_2 in the identity above, we deduce that

$$2\mu C_{k,1}\|\boldsymbol{u}\|^2_{1,\Omega} + \frac{c_0}{\alpha}\|p\|^2_{0,\Omega} \leq \|F_1\|_{\mathbf{H}'}\|\boldsymbol{u}\|_{1,\Omega} + \|G_2\|_{\mathrm{Q}'}\|p\|_{0,\Omega},$$

which implies that

$$\|\boldsymbol{u}\|_{1,\Omega} + \|p\|_{0,\Omega} \leq C_1(\|F_1\|_{\mathbf{H}'} + \|G_2\|_{\mathrm{Q}'}), \tag{2.27}$$

with $C_1 > 0$ independent of λ. Then from the first condition in (2.16) and (2.18) we observe that

$$\beta_s\|\phi\|_{0,\Omega} \leq \sup_{\boldsymbol{v}\in\mathbf{H}\setminus\{\mathbf{0}\}} \frac{b_s(\boldsymbol{v}, \phi)}{\|\boldsymbol{v}\|_{1,\Omega}} = \sup_{\boldsymbol{v}\in\mathbf{H}\setminus\{\mathbf{0}\}} \frac{F_1(v) - a_s(\boldsymbol{u}, \boldsymbol{v})}{\|\boldsymbol{v}\|_{1,\Omega}},$$

which together to (2.27) and the continuity of a_s and F_1, implies

$$\|\phi\|_{0,\Omega} \leq C_2(\|F_1\|_{\mathbf{H}'} + \|G_2\|_{\mathrm{Q}'}), \tag{2.28}$$

with $C_2 > 0$ independent of λ.

Now, in order to bound $\|\boldsymbol{\sigma}\|_{\mathrm{div},\Omega}$, we let $\boldsymbol{\sigma}_0 \in K_f$ and $\boldsymbol{\sigma}^\perp \in K_f^\perp$, such that $\boldsymbol{\sigma} = \boldsymbol{\sigma}_0 + \boldsymbol{\sigma}^\perp$. First, from (2.19) with $\boldsymbol{\tau} = \boldsymbol{\sigma}_0$ and noticing that $\boldsymbol{\sigma}_0 \in K_f$, we have

$$a_f(\boldsymbol{\sigma}_0, \boldsymbol{\sigma}_0) = -a_f(\boldsymbol{\sigma}^\perp, \boldsymbol{\sigma}_0),$$

which jointly with (2.15) and the continuity of a_f (cf. (2.11)), gives

$$\|\boldsymbol{\sigma}_0\|_{\mathrm{div},\Omega} \leq \frac{\kappa_2}{\kappa_1}\|\boldsymbol{\sigma}^\perp\|_{\mathrm{div},\Omega}. \tag{2.29}$$

In turn, combining the second condition in (2.16) with [13, Lemma 2.1] and (2.20), we obtain

$$\alpha^{-1}\beta_f\|\boldsymbol{\sigma}^\perp\|_{\mathrm{div},\Omega} \leq \sup_{q\in\mathrm{Q}\setminus\mathbf{0}} \frac{b_f(\boldsymbol{\sigma}, q)}{\|q\|_{0,\Omega}} = \sup_{q\in\mathrm{Q}\setminus\mathbf{0}} \frac{G_2(q) - b_{sf}(\phi, q) - c_f(p, q)}{\|q\|_{0,\Omega}},$$

which together to the continuity of G_2, b_{sf} and c_f (cf. (2.11)), estimates (2.27) and (2.28), yields

$$\|\boldsymbol{\sigma}^\perp\|_{\mathrm{div},\Omega} \leq C\left(\frac{1}{\alpha} + \frac{2}{\lambda} + \frac{C_0}{\alpha}\right)(\|F_1\|_{\mathbf{H}'} + \|G_2\|_{\mathrm{Q}'}), \tag{2.30}$$

where $\frac{1}{\alpha} + \frac{2}{\lambda} + \frac{C_0}{\alpha}$ must be thought as a constant independent of λ if $\lambda \to \infty$. Then, from (2.29), (2.30) and the triangle inequality we easily deduce that

$$\|\boldsymbol{\sigma}\|_{\mathrm{div},\Omega} \leq C_3(\|F_1\|_{\mathbf{H}'} + \|G_2\|_{\mathrm{Q}'}), \tag{2.31}$$

with $C_3 > 0$ independent of λ. We conclude the first step by observing that the aforementioned estimate follows from (2.27) (2.28) and (2.31).

Step 2 ($F_1 = 0$, $G_1 = 0$ and $G_2 = 0$): Now we proceed to bound the solution in terms of $\|F_2\|_{\mathbf{Z}'}$. To that end we recall the decomposition $F_2 = F_2^0 + F_2^\perp$ from (2.21). Consequently we bound the solution,

firstly in terms of $\|F_2^{\perp}\|_{(K_f^{\perp})'}$ (assuming that $F_2^0 = 0$), and secondly in terms of $\|F_2^0\|_{K_f'}$ (assuming that $F_2^{\perp} = 0$). Hence, the desired estimate follows by linearity, adding both estimates.

Let $\boldsymbol{\sigma}_0 \in K_f$ and $\boldsymbol{\sigma}^{\perp} \in K_f^{\perp}$ be such that $\boldsymbol{\sigma} = \boldsymbol{\sigma}_0 + \boldsymbol{\sigma}^{\perp}$. Similarly, we let $\boldsymbol{u}_0 \in K_s$ and $\boldsymbol{u}^{\perp} \in K_s^{\perp}$ be such that $\boldsymbol{u} = \boldsymbol{u}_0 + \boldsymbol{u}^{\perp}$. In turn, taking $\boldsymbol{v} = \boldsymbol{u}$ in (2.17), $\psi = \phi$ in (2.18), $\boldsymbol{\tau} = \boldsymbol{\sigma}$ in (2.19) and $q = p$ in (2.20) and performing the operations (2.17) − (2.18) + (2.19) − (2.20), we observe that there holds

$$a_s(\boldsymbol{u}, \boldsymbol{u}) + a_f(\boldsymbol{\sigma}, \boldsymbol{\sigma}) + C((\phi, p), (\phi, p)) = F_2^0(\boldsymbol{\sigma}_0) + F_2^{\perp}(\boldsymbol{\sigma}^{\perp}), \tag{2.32}$$

In addition, from (2.19) with $\boldsymbol{\tau} = \boldsymbol{\sigma}_0$ and (2.22) we notice that

$$a_f(\boldsymbol{\sigma}_0, \boldsymbol{\sigma}_0) + a_f(\boldsymbol{\sigma}^{\perp}, \boldsymbol{\sigma}_0) = F_2^0(\boldsymbol{\sigma}_0). \tag{2.33}$$

$\underline{F_2^0 = 0}$: We begin by noticing that from (2.32) there holds

$$C((\phi, p), (\phi, p)) \leq F_2^{\perp}(\boldsymbol{\sigma}^{\perp}), \tag{2.34}$$

and since $F_2^0 = 0$, from (2.33), and from the continuity and ellipticity of a_f, we have

$$\|\boldsymbol{\sigma}_0\|_{\mathrm{div},\Omega} \leq \frac{\kappa_2}{\kappa_1} \|\boldsymbol{\sigma}^{\perp}\|_{\mathrm{div},\Omega}. \tag{2.35}$$

Moreover, summing up equations (2.18) and (2.20), we deduce that

$$b_s(\boldsymbol{u}^{\perp}, \psi) + b_f(\boldsymbol{\sigma}^{\perp}, q) = C((\phi, p), (\psi, q)) \quad \forall\, \psi, q \in \mathrm{Q},$$

which together to (2.24), (2.25) and (2.34) implies

$$\begin{aligned}
\beta \|\boldsymbol{\sigma}^{\perp}\|_{\mathrm{div},\Omega} &\leq \sup_{(\psi,q)\in(\mathrm{Q}\times\mathrm{Q})\setminus\mathbf{0}} \frac{b_s(\boldsymbol{u}^{\perp}, \psi) + b_f(\boldsymbol{\sigma}^{\perp}, q)}{\|\psi\|_{0,\Omega} + \|q\|_{0,\Omega}} = \sup_{(\psi,q)\in(\mathrm{Q}\times\mathrm{Q})\setminus\mathbf{0}} \frac{C((\phi, p), (\psi, q))}{\|\psi\|_{0,\Omega} + \|q\|_{0,\Omega}} \\
&\leq \left(\frac{1}{\lambda} \|\phi - p\|_{0,\Omega}^2 + \frac{c_0}{\alpha} \|p\|_{0,\Omega}^2 \right)^{1/2} \sup_{(\psi,q)\in(\mathrm{Q}\times\mathrm{Q})\setminus\mathbf{0}} \frac{\left(\frac{1}{\lambda} \|\psi - q\|_{0,\Omega}^2 + \frac{c_0}{\alpha} \|q\|_{0,\Omega}^2 \right)^{1/2}}{\|\psi\|_{0,\Omega} + \|q\|_{0,\Omega}} \\
&\leq \left(F_2^{\perp}(\boldsymbol{\sigma}^{\perp}) \right)^{1/2} \sup_{(\psi,q)\in(\mathrm{Q}\times\mathrm{Q})\setminus\mathbf{0}} \frac{\left(\frac{1}{\lambda} \|\psi - q\|_{0,\Omega}^2 + \frac{c_0}{\alpha} \|q\|_{0,\Omega}^2 \right)^{1/2}}{\|\psi\|_{0,\Omega} + \|q\|_{0,\Omega}}.
\end{aligned} \tag{2.36}$$

Then, defining

$$C_c = \sup_{(\psi,q)\in(\mathrm{Q}\times\mathrm{Q})\setminus\mathbf{0}} \frac{\left(\frac{1}{\lambda} \|\psi - q\|_{0,\Omega}^2 + \frac{c_0}{\alpha} \|q\|_{0,\Omega}^2 \right)^{1/2}}{\|\psi\|_{0,\Omega} + \|q\|_{0,\Omega}}, \tag{2.37}$$

which can be seen as a constant independent of λ if $\lambda \to \infty$, from (2.36) we obtain

$$\|\boldsymbol{\sigma}^{\perp}\|_{\mathrm{div},\Omega} \leq \frac{C_c^2}{\beta^2} \|F_2^{\perp}\|_{(K_f^{\perp})'}. \tag{2.38}$$

Hence, combining (2.32) and (2.38) together to (2.14) we can easily deduce that

$$\|\boldsymbol{u}\|_{1,\Omega} + \|p\|_{0,\Omega} \leq C_4 \|F_2^{\perp}\|_{(K_f^{\perp})'}, \tag{2.39}$$

with $C_4 > 0$ independent of λ. Moreover, from (2.35), (2.38) and the triangle inequality we also get

$$\|\boldsymbol{\sigma}\|_{\mathrm{div},\Omega} \leq \|\boldsymbol{\sigma}_0\|_{\mathrm{div},\Omega} + \|\boldsymbol{\sigma}^{\perp}\|_{\mathrm{div},\Omega} \leq \left(1 + \frac{\kappa_2}{\kappa_1} \right) \|\boldsymbol{\sigma}^{\perp}\|_{\mathrm{div},\Omega} \leq C_5 \|F_2^{\perp}\|_{(K_f^{\perp})'}, \tag{2.40}$$

with $C_5 > 0$ independent of λ. Finally, using the inf-sup condition (2.16) and proceeding similarly as for the derivation of (2.28), we can obtain

$$\|\phi\|_{0,\Omega} \leq C_6 \|F_2^{\perp}\|_{(K_f^{\perp})'} \tag{2.41}$$

with $C_6 > 0$ independent of λ. In this way from (2.39)-(2.41) we obtain the result for the case $F_2^0 = 0$.

$F_2^\perp = 0$: First, from (2.32) and (2.33) we obtain, respectively

$$\frac{1}{\lambda}\|\phi - p\|_{0,\Omega}^2 + \frac{c_0}{\alpha}\|p\|_{0,\Omega}^2 \leq F_2^0(\boldsymbol{\sigma}_0), \tag{2.42}$$

and

$$\|\boldsymbol{\sigma}_0\|_{\mathrm{div},\Omega} \leq \frac{\kappa_2}{\kappa_1}\|\boldsymbol{\sigma}^\perp\|_{\mathrm{div},\Omega} + \frac{2\kappa_2\alpha}{\eta}\|F_2^0\|_{K_f'}. \tag{2.43}$$

Now, similarly as in (2.36), from the inf-sup condition (2.24), estimates (2.25) and (2.42), and recalling the definition of the constant C_c in (2.37), we obtain

$$\beta\|\boldsymbol{\sigma}^\perp\|_{\mathrm{div},\Omega} \leq C_c\left(F_2^0(\boldsymbol{\sigma}_0)\right)^{1/2} \leq C_c\|F_2^0\|_{K_f'}^{1/2}\|\boldsymbol{\sigma}_0\|_{\mathrm{div},\Omega}^{1/2},$$

which, associated with (2.43) and Young's inequality, yields

$$\|\boldsymbol{\sigma}^\perp\|_{\mathrm{div},\Omega} \leq C\|F_2^0\|_{K_f'} + \tilde{C}\|F_2^0\|_{K_f'}^{1/2}\|\boldsymbol{\sigma}^\perp\|_{\mathrm{div},\Omega}^{1/2} \leq \hat{C}\|F_2^0\|_{K_f'} + \frac{1}{2}\|\boldsymbol{\sigma}^\perp\|_{\mathrm{div},\Omega},$$

and therefore

$$\|\boldsymbol{\sigma}^\perp\|_{\mathrm{div},\Omega} \leq 2\hat{C}\|F_2^0\|_{K_f'}, \tag{2.44}$$

with $\hat{C}$ independent of λ. Notice that from the latter and estimate (2.43) it readily follows that

$$\|\boldsymbol{\sigma}_0\|_{\mathrm{div},\Omega} \leq \bar{C}\|F_2^0\|_{K_f'}. \tag{2.45}$$

In this way, from (2.44), (2.45) and the triangle inequality, we can assert that

$$\|\boldsymbol{\sigma}\|_{\mathrm{div},\Omega} \leq C_7\|F_2^0\|_{K_f'}, \tag{2.46}$$

with $C_7 > 0$ independent of λ. Moreover, from (2.14), (2.32) and (2.45) we can deduce that

$$\|\boldsymbol{u}\|_{1,\Omega} + \|p\|_{0,\Omega} \leq C_8\|F_2^0\|_{K_f'}, \tag{2.47}$$

with $C_8 > 0$ independent of λ, and to conclude, analogously to (2.28), from the inf-sup condition (2.16), equation (2.18) and (2.47), we obtain

$$\|\phi\|_{0,\Omega} \leq C_9\|F_2^0\|_{K_f'}, \tag{2.48}$$

with $C_9 > 0$ independent of λ. The desired estimate then follows from (2.46)-(2.48).

Step 3 ($F_1 = 0$, G_2 and $F_2 = 0$): Once again we let $\boldsymbol{\sigma}_0 \in K_f$ and $\boldsymbol{\sigma}^\perp \in K_f^\perp$ be such that $\boldsymbol{\sigma} = \boldsymbol{\sigma}_0 + \boldsymbol{\sigma}^\perp$ and $\boldsymbol{u}_0 \in K_s$ and $\boldsymbol{u}^\perp \in K_s^\perp$ satisfying $\boldsymbol{u} = \boldsymbol{u}_0 + \boldsymbol{u}^\perp$, and observe that there holds

$$a_s(\boldsymbol{u},\boldsymbol{u}) + a_f(\boldsymbol{\sigma},\boldsymbol{\sigma}) + C((\phi,p),(\phi,p)) = G_1(\phi), \tag{2.49}$$

and

$$b_s(\boldsymbol{u}^\perp,\psi) + b_f(\boldsymbol{\sigma}^\perp,q) - C((\phi,p),(\psi,q)) = G_1(\psi) \quad \forall\, \psi, q \in \mathrm{Q}.$$

In particular, from the latter and the inf-sup condition (2.16) we obtain

$$\begin{aligned}\beta(\|\boldsymbol{u}^\perp\|_{1,\Omega} + \|\boldsymbol{\sigma}^\perp\|_{\mathrm{div},\Omega}) &\leq \sup_{(\psi,q)\in(\mathrm{Q}\times\mathrm{Q})\setminus\mathbf{0}} \frac{b_s(\boldsymbol{u}^\perp,\psi) + b_f(\boldsymbol{\sigma}^\perp,q)}{\|\psi\|_{0,\Omega} + \|q\|_{0,\Omega}} \\ &= \sup_{(\psi,q)\in(\mathrm{Q}\times\mathrm{Q})\setminus\mathbf{0}} \frac{G_1(\psi) + C((\phi,p),(\psi,q))}{\|\psi\|_{0,\Omega} + \|q\|_{0,\Omega}},\end{aligned}$$

which together with (2.25), (2.49) and the continuity of G_1, gives the bound

$$\begin{aligned}\beta(\|\boldsymbol{u}^{\perp}\|_{1,\Omega}+\|\boldsymbol{\sigma}^{\perp}\|_{\mathrm{div},\Omega}) \leq & \|G_1\|_{\mathrm{Q}'}+C_c\{C((\phi,p),(\phi,p))\}^{1/2}\\ \leq & \|G_1\|_{\mathrm{Q}'}+C_c\|G_1\|_{\mathrm{Q}'}^{1/2}\|\phi\|_{0,\Omega}^{1/2}.\end{aligned} \tag{2.50}$$

where $C_c>0$ is the constant defined in (2.37). Now, from (2.17) with $\boldsymbol{v}=\boldsymbol{u}_0$ and using the ellipticity and continuity of a_s (cf. (2.14) and (2.11), respectively), it readily follows that

$$\|\boldsymbol{u}_0\|_{1,\Omega}\leq\frac{C_{k,2}}{C_{k,1}}\|\boldsymbol{u}^{\perp}\|_{1,\Omega},$$

which implies

$$\|\boldsymbol{u}\|_{1,\Omega}\leq\left(1+\frac{C_{k,2}}{C_{k,1}}\right)\|\boldsymbol{u}^{\perp}\|_{1,\Omega}. \tag{2.51}$$

The latter, the inf-sup condition (2.16) and equation (2.17) yield

$$\|\phi\|_{0,\Omega}\leq\beta_s^{-1}\sup_{\boldsymbol{v}\in\mathbf{H}\setminus\mathbf{0}}\frac{b_s(\boldsymbol{v},\phi)}{\|\boldsymbol{v}\|_{1,\Omega}}\leq\beta_s^{-1}\sup_{\boldsymbol{v}\in\mathbf{H}\setminus\mathbf{0}}\frac{-a_s(\boldsymbol{u},\boldsymbol{v})}{\|\boldsymbol{v}\|_{1,\Omega}}\leq 2\mu\beta_s^{-1}C_{k,2}\|\boldsymbol{u}\|_{1,\Omega}\leq\hat{C}_1\|\boldsymbol{u}^{\perp}\|_{1,\Omega}, \tag{2.52}$$

with $\hat{C}_1>0$ independent of λ. Then, combining (2.50) and (2.52) with Young's inequality, we obtain

$$\|\boldsymbol{u}^{\perp}\|_{1,\Omega}\leq\hat{C}_2\|G_1\|_{\mathrm{Q}'}.$$

Using this inequality, from (2.51) and (2.52), we easily get

$$\|\boldsymbol{u}\|_{1,\Omega}\leq\hat{C}_3\|G_1\|_{\mathrm{Q}'}\quad\text{and}\quad\|\phi\|_{0,\Omega}\leq\hat{C}_4\|G_1\|_{\mathrm{Q}'}, \tag{2.53}$$

with $\hat{C}_3>0$ and $\hat{C}_4>0$ independent of λ. In turn, similarly as in (2.29) we can assert that

$$\|\boldsymbol{\sigma}_0\|_{\mathrm{div},\Omega}\leq\frac{\kappa_2}{\kappa_1}\|\boldsymbol{\sigma}^{\perp}\|_{\mathrm{div},\Omega},$$

and invoking (2.50) and (2.53) we can derive the bound

$$\|\boldsymbol{\sigma}\|_{\mathrm{div},\Omega}\leq\hat{C}_5\|G_1\|_{\mathrm{Q}'}, \tag{2.54}$$

with $\hat{C}_5>0$ independent of λ. Finally, from the second inf-sup condition in (2.16), equation (2.19) and estimate (2.54) there holds

$$\|p\|_{0,\Omega}\leq\hat{C}_6\|G_1\|_{\mathrm{Q}'}. \tag{2.55}$$

In this way, from (2.53), (2.54) and (2.55) we obtain the desired estimate, which concludes the proof. □

As a consequence of Theorem 2.1 we can readily deduce the following result.

Theorem 2.2 *There exists a unique* $(\boldsymbol{u},\phi,\boldsymbol{\sigma},p)\in\mathbf{H}\times\mathrm{Q}\times\mathbf{Z}\times\mathrm{Q}$ *satisfying* (2.6)–(2.9). *Moreover, there exists* $C>0$, *independent of* λ, *such that*

$$\|\boldsymbol{u}\|_{1,\Omega}+\|\phi\|_{0,\Omega}+\|\boldsymbol{\sigma}\|_{\mathrm{div},\Omega}+\|p\|_{0,\Omega}\leq C_{stab}(\|\boldsymbol{f}\|_{0,\Omega}+\|\boldsymbol{g}\|_{0,\Omega}+\|\ell\|_{0,\Omega}+\|p_{\Gamma}\|_{1/2,00,\Gamma_p}).$$

Proof. By setting $F_1,F_2=0$ and $G_1,G_2=0$ in (2.17)–(2.20) from Theorem 2.1 we can readily deduce the uniqueness of solution of problem (2.6)–(2.9). Furthermore, noticing that (2.6)–(2.9) is a symmetric linear problem, the above also guarantees existence of solution, which completes the solvability analysis. In turn, by setting $F_1=F$, $G_1=0$, $F_2=G$ and $G_2=H$, the continuous dependence result is a direct consequence of Theorem 2.1 and (2.12), which concludes the proof. □

3 Discontinuous finite volumes - mixed finite elements

Primal and dual meshes. The construction of DFV-MFE schemes can be straightforwardly carried out for $d = 2, 3$; however, for sake of conciseness, we will restrict the presentation to the 2D case. Let us then consider a family $\{\mathcal{T}_h\}_{h>0}$ of regular, quasi-uniform partitions of $\bar{\Omega}$ into triangles T of diameter h_T, where $h = \max\{h_T : T \in \mathcal{T}_h\}$ is the meshsize. We will refer to these triangulations as *primal meshes*.

Let $\mathcal{E}_h$ denote the set of interior edges in the primal mesh and write $\mathcal{E}_h(T)$ for its localisation to the element $T \in \mathcal{T}_h$. Moreover, let $e \in \mathcal{E}_h$ be shared by two elements T_1 and T_2 in $\mathcal{T}_h$ with outward unit normal vectors $\boldsymbol{n}_1$ and $\boldsymbol{n}_2$, respectively. For a scalar q, we will write $[\![q]\!] := q|_{\partial T_1} - q|_{\partial T_2}$ and $\{\!\{q\}\!\} := \frac{1}{2}(q|_{\partial T_1} + q|_{\partial T_2})$ to denote its jump and average values on e, respectively. For a generic vector $\mathbf{r}$, its vector jump and vectorial average across edge e is denoted respectively, by $[\![\mathbf{r}]\!] := \mathbf{r}|_{\partial T_1} - \mathbf{r}|_{\partial T_2}$ and $\{\!\{\mathbf{r}\}\!\} := \frac{1}{2}(\mathbf{r}|_{\partial T_1} + \mathbf{r}|_{\partial T_2})$.

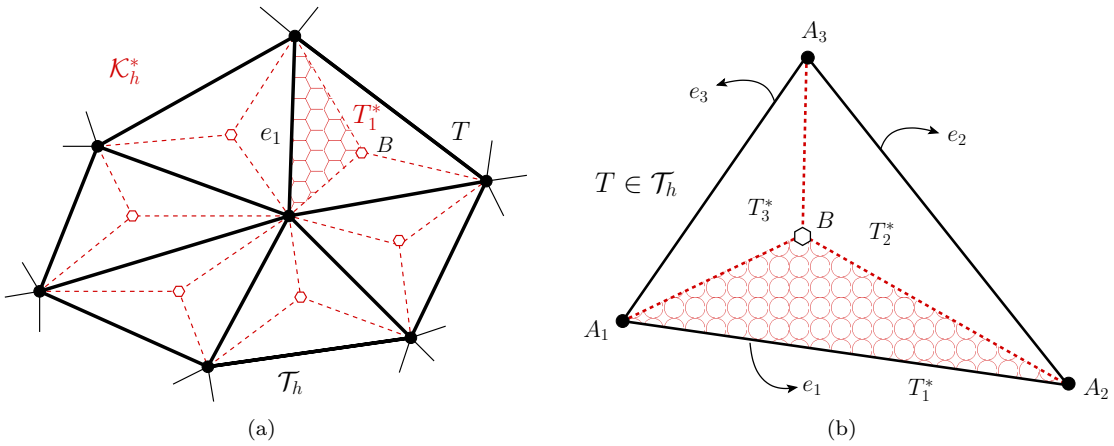

Figure 1: A compound of six elements in $\mathcal{T}_h$ (a), and barycentric subdivision of a given $T \in \mathcal{T}_h$ into three control volumes T_j^* belonging to the dual mesh $\mathcal{K}_h^*$ (b). The vertices of $\mathcal{T}_h$ are labelled with A_i, and the edges of primal elements are denoted e_i.

In order to define DFV approximations for the solid displacements, we construct an auxiliary, *dual mesh*. Starting from a given triangle T in the primal mesh $\mathcal{T}_h$, we proceed to divide it into three sub-triangles by joining the barycentre B to the vertices of T. The dual mesh, denoted by $\mathcal{K}_h^*$, will then consist of all these *control volumes*, T^*, generated after barycentric subdivison. A sketch of the subdivision in a given T and also a compound of six primal elements is presented in Figure 1.

Discrete trial and test spaces. Specifying the trial and test spaces will completely characterise the DFV method. Let us introduce the trial space for the approximation of solid displacements as

$$\mathbf{H}_h := \{\boldsymbol{v}_h \in \mathbf{L}^2(\Omega) : \boldsymbol{v}_h|_T \in \mathcal{P}_1(T)^2 \quad \forall T \in \mathcal{T}_h\},$$

whereas the corresponding test space will be associated to the dual mesh $\mathcal{K}_h^*$, and will be defined as

$$\mathbf{H}_h^* := \{\boldsymbol{v}_h \in \mathbf{L}^2(\Omega) : \boldsymbol{v}_h|_T^* \in \mathcal{P}_0(T^*)^2 \quad \forall T^* \in \mathcal{K}_h^*\}.$$

Here $\mathcal{P}_k(T)$ denotes the space of polynomials of degree less than or equal than k defined over the element T. One readily notices that given the specific form of control volumes, the linear systems arising from the discretisation of operators involving the solid displacement approximation will be square. Moreover, we observe that the dual elements have support only in the primal triangle they belong to (in contrast to conforming FVE schemes, where the control volumes have a support shared

on the neighbouring triangles in the primal mesh). Such localisation property may turn the method more amenable for parallelisation and eventual implementation of adaptive DFV schemes.

Next, let us define a space having higher regularity $\mathbf{H}(h) := \mathbf{H}_h + [\mathbf{H}^2(\Omega) \cap \mathbf{H}^1_{\Gamma_{\boldsymbol{u}}}(\Omega)]$, and introduce a mapping that connects this modified trial space with the test space as follows

$$R_h : \mathbf{H}(h) \longrightarrow \mathbf{H}_h^*, \qquad \boldsymbol{v}|_{T^*} \mapsto R_h \boldsymbol{v}|_{T^*} := \frac{1}{h_e} \int_e \boldsymbol{v}|_{T^*}, \quad T^* \in \mathcal{K}_h^*,$$

where h_e denotes the length of the generic edge e of the primal element T that contains the control volume T^* (see Figure 1(b)). We provide $\mathbf{H}(h)$ with the mesh-dependent norm $|||\cdot|||_h$, defined as

$$|||\boldsymbol{v}|||_h^2 := |\boldsymbol{v}|_{1,h}^2 + \sum_{e \in \mathcal{E}_h} \frac{1}{h_e} \int_e [\![\boldsymbol{v}]\!]^2,$$

which uses the broken $\mathbf{H}-$semi-norm $|\boldsymbol{v}|_{1,h}^2 = \sum\limits_{T \in \mathcal{T}_h} |\boldsymbol{v}|_{1,T}^2$.

On the other hand, we consider the finite dimensional space associated with the approximation of the fluid flux and the fluid pressure as the mixed finite element constituted by the lowest order Raviart-Thomas space and the space of piecewise constants defined over the primal mesh

$$\begin{aligned} \mathbf{Z}_h &:= \{\boldsymbol{\tau}_h \in \mathbf{Z} : \boldsymbol{\tau}_h|_T \in \mathcal{RT}_0(T), \, \forall T \in \mathcal{T}_h, \text{ and } \boldsymbol{\tau}_h \cdot \boldsymbol{n} = 0 \text{ on } \Gamma_{\boldsymbol{u}}\}, \\ \mathrm{Q}_h &:= \{q_h \in \mathrm{Q} : q_h|_T \text{ is a constant}, \, \forall T \in \mathcal{T}_h\}, \end{aligned}$$

where $\mathcal{RT}_0$ denotes the local Raviart-Thomas space of lowest order. The trial and test spaces for the approximation of the total pressure will coincide with the ones used for the fluid pressure.

The conservative discrete formulation. Applying then a combined DFV-MFE discretisation, we end up with the following formulation: Find $(\boldsymbol{u}_h, \phi_h, \boldsymbol{\sigma}_h, p_h) \in \mathbf{H}_h \times \mathrm{Q}_h \times \mathbf{Z}_h \times \mathrm{Q}_h$ such that

$$a_s^h(\boldsymbol{u}_h, \boldsymbol{v}_h) + b_s^h(\boldsymbol{v}_h, \phi_h) = F(R_h \boldsymbol{v}_h) \quad \forall \boldsymbol{v}_h \in \mathbf{H}_h, \tag{3.1}$$

$$\tilde{b}_s^h(\boldsymbol{u}_h, \psi_h) - c_s(\phi_h, \psi_h) + b_{sf}(\psi_h, p_h) = 0 \quad \forall \psi_h \in \mathrm{Q}_h, \tag{3.2}$$

$$a_f(\boldsymbol{\sigma}_h, \boldsymbol{\tau}_h) + b_f(\boldsymbol{\tau}_h, p_h) = G(\boldsymbol{\tau}_h) \quad \forall \boldsymbol{\tau}_h \in \mathbf{Z}_h, \tag{3.3}$$

$$b_{sf}(\phi_h, q_h) + b_f(\boldsymbol{\sigma}_h, q_h) - c_f(p_h, q_h) = H(q_h) \quad \forall q_h \in \mathrm{Q}_h, \tag{3.4}$$

where the three bilinear forms that are modified with respect to the ones specified in (2.10), are now defined as follows

$$\begin{aligned} a_s^h(\boldsymbol{u}_h, \boldsymbol{v}_h) := &- 2\mu \sum_{\mathcal{T} \in \mathcal{T}_h} \sum_{j=1}^{3} \int_{A_{j+1}BA_j} \boldsymbol{\varepsilon}(\boldsymbol{u}_h)\boldsymbol{n} \cdot R_h \boldsymbol{v}_h - 2\mu \sum_{e \in \mathcal{E}_h} \langle [\![R_h \boldsymbol{v}_h]\!], \{\!\{\boldsymbol{\varepsilon}(\boldsymbol{u}_h)\boldsymbol{n}\}\!\} \rangle_e \\ &- 2\theta\mu \sum_{e \in \mathcal{E}_h \cup \Gamma_{\boldsymbol{u}}} \langle [\![R_h \boldsymbol{u}_h]\!], \{\!\{\varepsilon(\boldsymbol{v}_h)\boldsymbol{n}\}\!\} \rangle_e + \sum_{e \in \mathcal{E}_h \cup \Gamma_{\boldsymbol{u}}} 2\mu \frac{\gamma_{\boldsymbol{u}}}{h_e} \langle [\![R_h \boldsymbol{u}_h]\!], [\![R_h \boldsymbol{v}_h]\!] \rangle_e, \\ b_s^h(\boldsymbol{v}_h, \psi_h) := &\sum_{\mathcal{T} \in \mathcal{T}_h} \sum_{j=1}^{3} \int_{A_{j+1}BA_j} \psi_h R_h \boldsymbol{v}_h \cdot \boldsymbol{n} + \sum_{e \in \mathcal{E}_h} \langle \{\!\{\psi_h \boldsymbol{n}\}\!\}, [\![R_h \boldsymbol{v}_h]\!] \rangle_e, \\ \tilde{b}_s^h(\boldsymbol{u}_h, \psi_h) := &- \int_\Omega \psi_h \operatorname{div} \boldsymbol{u}_h + \sum_{e \in \mathcal{E}_h \cup \Gamma_{\boldsymbol{u}}} \langle \{\!\{\psi_h \boldsymbol{n}\}\!\}, [\![R_h \boldsymbol{u}_h]\!] \rangle_e, \end{aligned}$$

with $A_4 = A_1$ (see Figure 1(b)), and where $\gamma_{\boldsymbol{u}} > 0$ and $\gamma_\phi > 0$ are penalty parameters independent of h (see e.g. the DFV formulations for Stokes equations proposed in [17, 33]). The symmetrisation parameter $\theta \in \{1, 0, -1\}$ leads respectively to symmetric, incomplete, and non-symmetric interior penalty DG formulations. We recall that for boundary edges we adopt the convention that $\{\!\{\mathbf{r}\}\!\} = \mathbf{r}$ and $[\![\mathbf{r}]\!] = \mathbf{r}$, for a generic vector field $\mathbf{r}$. We also note that the edge integrals on $\Gamma_{\boldsymbol{u}}$ are required only if the Dirichlet boundary conditions for displacements are implemented using Nitsche's approach.

4 Solvability and stability of the discrete problem

Preliminaries. The unique solvability of the discrete problem (3.1)-(3.4) can be established by proving that the sole feasible solution to the homogeneous counterpart of the system is the trivial one. We start by collecting some useful results to be exploited in the sequel.

First, for any $\boldsymbol{v} \in \mathbf{H}^2(T)$ and for any edge $e \in \mathcal{E}_h(T)$ one has the trace inequality (cf. [2])

$$\|\boldsymbol{v}\|_{0,e}^2 \leq C \left(h_e^{-1} \|\boldsymbol{v}\|_{0,T}^2 + h_e |\boldsymbol{v}|_{1,T}^2 \right). \tag{4.1}$$

Secondly, the bilinear forms $a_s^h(\cdot,\cdot)$, $\tilde{b}_1^h(\cdot,\cdot)$ and $b_1^h(\cdot,\cdot)$ hold the following set of properties (continuity, positivity, and suitable inf-sup conditions). There exist constants $C_i > 0, \beta_0 > 0$ independent of the meshsize h, such that

$$a_s^h(\boldsymbol{v}_h, \boldsymbol{w}_h) \leq C_1 \, |\!|\!| \boldsymbol{v}_h |\!|\!|_h \, |\!|\!| \boldsymbol{w}_h |\!|\!|_h \qquad \forall \boldsymbol{v}_h, \boldsymbol{w}_h \in \mathbf{H}(h), \tag{4.2}$$

$$a_s^h(\boldsymbol{v}_h, \boldsymbol{v}_h) \geq C_2 \, |\!|\!| \boldsymbol{v}_h |\!|\!|_h^2 \qquad \forall \boldsymbol{v}_h \in \mathbf{H}_h, \tag{4.3}$$

$$b_s^h(\boldsymbol{v}_h, \psi_h) \leq C_3 \, |\!|\!| \boldsymbol{v}_h |\!|\!|_h \left[\|\psi_h\|_{0,\Omega} + \left(\sum_{T \in \mathcal{T}_h} h_T^2 |\psi_h|_{1,T}^2 \right)^{\frac{1}{2}} \right] \qquad \forall \boldsymbol{v}_h \in \mathbf{H}(h), \, \psi_h \in \mathrm{Q}_h, \tag{4.4}$$

$$\sup_{0 \neq \boldsymbol{v}_h \in \mathbf{H}_h} \frac{\tilde{b}_s^h(\boldsymbol{v}_h, \psi_h)}{|\!|\!| \boldsymbol{v}_h |\!|\!|_h} \geq \beta_0 \, \|\psi_h\|_{0,\Omega} \qquad \forall \psi_h \in \mathrm{Q}_h, \tag{4.5}$$

$$b_s^h(\boldsymbol{v}_h, \psi_h) = \tilde{b}_s^h(\boldsymbol{v}_h, \psi_h) \qquad \boldsymbol{v}_h \in \mathbf{H}(h), \psi_h \in \mathrm{Q}_h. \tag{4.6}$$

For a proof of (4.2)-(4.3) we refer to [17, Lemma 4], whereas the bounds (4.4), (4.5), as well as the equivalence (4.6) can be found respectively in [33, Lemmas 3.4, 4.1 & 3.2]. In particular, from (4.4) and the inverse inequality $|\psi_h|_{1,T} \leq C h^{-1} \|\psi_h\|_{0,T}$, for all $\phi_h \in \mathrm{Q}_h$ and for all $T \in \mathcal{T}_h$, with $C > 0$ independent of h (see for instance [11, Lemma 1.44]), it follows that

$$b_s^h(\boldsymbol{v}_h, \psi_h) \leq \widetilde{C}_3 \, |\!|\!| \boldsymbol{v}_h |\!|\!|_h \, \|\psi_h\|_{0,\Omega} \quad \forall \, \boldsymbol{v}_h \in \mathbf{H}(h), \, \psi_h \in \mathrm{Q}_h. \tag{4.7}$$

Let us now establish the stability properties of the forms a_f, b_f and c_f. We begin by recalling that, since $\operatorname{div} \mathbf{Z}_h \subseteq \mathrm{Q}_h$, the kernel of the bilinear form b_f can be characterised as follows

$$\mathbf{K}_h := \{\boldsymbol{\tau}_h \in \mathbf{Z}_h \ : \ b_f(\boldsymbol{\tau}_h, q_h) = 0 \quad \forall \, q_h \in \mathrm{Q}_h\} = \{\boldsymbol{\tau}_h \in \mathbf{Z}_h \ : \ \operatorname{div} \boldsymbol{\tau}_h = 0 \qquad \text{in} \quad \Omega\}.$$

Then, the $\mathbf{K}_h$–ellipticity of the bilinear form a_f is straightforward

$$a_f(\boldsymbol{\tau}_h, \boldsymbol{\tau}_h) \geq \frac{\eta}{\kappa \alpha} \|\boldsymbol{\tau}_h\|_{\operatorname{div},\Omega}^2 \qquad \forall \, \boldsymbol{\tau}_h \in \mathbf{K}_h.$$

In turn, it is well–known that the bilinear form b_f satisfies the following inf–sup condition

$$\sup_{\boldsymbol{\tau}_h \in \mathbf{Z}_h \setminus \{\mathbf{0}\}} \frac{b_f(\boldsymbol{\tau}_h, q_h)}{\|\boldsymbol{\tau}_h\|_{\operatorname{div},\Omega}} \geq \widehat{\beta} \|q_h\|_{0,\Omega} \qquad \forall \, q_h \in \mathrm{Q}_h,$$

with $\widehat{\beta} > 0$ independent of h (see [13, Section 4.2]).

We point out that the continuity of the forms c_s, b_{sf}, a_f, b_f, c_f, as well as the functionals G and H are inherited from the continuous case, preserving the exact same continuity constants.

Well-posedness of the discrete scheme. We proceed similarly to the continuous case, and establish continuous dependence on data for (3.1)–(3.4) considering generic functionals, that is, we let $F_1^h \in \mathbf{H}_h'$, $G_1^h \in \mathrm{Q}_h'$, $F_2^h \in \mathbf{Z}_h'$ and $G_2^h \in \mathrm{Q}_h'$ and bound $\boldsymbol{u}_h \in \mathbf{H}_h$, $\phi_h \in \mathrm{Q}_h$, $\boldsymbol{\sigma}_h \in \mathbf{Z}_h$ and $p_h \in \mathrm{Q}_h$, satisfying

$$a_s^h(\boldsymbol{u}_h, \boldsymbol{v}_h) + b_s^h(\boldsymbol{v}_h, \phi_h) = F_1^h(\boldsymbol{v}_h) \quad \forall \boldsymbol{v}_h \in \mathbf{H}_h, \tag{4.8}$$

$$\tilde{b}_s^h(\boldsymbol{u}_h,\psi_h) - c_s(\phi_h,\psi_h) + b_{sf}(\psi_h,p_h) = G_1^h(\psi_h) \quad \forall \psi_h \in \mathrm{Q}_h, \tag{4.9}$$

$$a_f(\boldsymbol{\sigma}_h,\boldsymbol{\tau}_h) + b_f(\boldsymbol{\tau}_h,p_h) = F_2^h(\boldsymbol{\tau}_h) \quad \forall \boldsymbol{\tau}_h \in \mathbf{Z}_h, \tag{4.10}$$

$$b_{sf}(\phi_h,q_h) + b_f(\boldsymbol{\sigma}_h,q_h) - c_f(p_h,q_h) = G_2^h(q_h) \quad \forall q_h \in \mathrm{Q}_h, \tag{4.11}$$

in terms of the aforementioned functionals F_1^h, G_1^h, F_2^h and G_2^h. This result is established next.

Theorem 4.1 *Let $(\boldsymbol{u},\phi,\boldsymbol{\sigma},p) \in \mathbf{H}\times\mathrm{Q}\times\mathbf{Z}\times\mathrm{Q}$ satisfy the system of equations (4.8)–(4.11). Then, there exists a constant $\widehat{C}>0$, independent of h and λ, such that*

$$|||\boldsymbol{u}_h|||_h + \|\phi_h\|_{0,\Omega} + \|\boldsymbol{\sigma}_h\|_{\mathrm{div},\Omega} + \|p_h\|_{0,\Omega} \leq \widehat{C}(\|F_1^h\|_{\mathbf{H}_h'} + \|G_1^h\|_{\mathrm{Q}_h'} + \|F_2^h\|_{\mathbf{Z}_h'} + \|G_2^h\|_{\mathrm{Q}_h'}). \tag{4.12}$$

Proof. Employing the discrete version of the stability properties of the forms involved, and proceeding analogously to the proof of Theorem 2.1, we can straightforwardly derive (4.12). □

Now we are in position of establishing the well-posedness and stability of (3.1)–(3.4).

Theorem 4.2 *There exists a unique $(\boldsymbol{u}_h,\phi_h,\boldsymbol{\sigma}_h,p_h) \in \mathbf{H}_h\times\mathrm{Q}_h\times\mathbf{Z}_h\times\mathrm{Q}_h$ solution of the system (3.1)–(3.4). Moreover, there exists a constant $\widehat{C}_{stab}>0$, independent of λ, such that*

$$|||\boldsymbol{u}_h|||_h + \|\phi_h\|_{0,\Omega} + \|\boldsymbol{\sigma}_h\|_{\mathrm{div},\Omega} + \|p_h\|_{0,\Omega} \leq \widehat{C}_{stab}(\|\boldsymbol{f}\|_{0,\Gamma} + \|\boldsymbol{g}\|_{0,\Omega} + \|\ell\|_{0,\Omega} + \|p_\Gamma\|_{1/2,00,\Gamma_p}). \tag{4.13}$$

Proof. By setting $F_1^h=0$, $G_1^h=0$, $F_2^h=0$ and $G_2^h=0$ in (4.8)–(4.11) from Theorem 4.1 it follows that $\boldsymbol{u}_h=\mathbf{0}$, $\phi_h=0$, $\boldsymbol{\sigma}_h=\mathbf{0}$ and $p_h=0$ which implies that that the only solution of the homogeneous problem is the trivial solution. From the latter, and from the fact that for finite dimensional linear problems existence and uniqueness of solution are equivalent, we readily obtain the well-posedness of (3.1)–(3.4). Moreover, by setting $F_1^h = FR_h|_{\mathbf{H}_h}$, $G_1^h=0$, $F_2^h = G|_{\mathbf{Z}_h}$ and $G_2^h = H|_{\mathrm{Q}_h}$ in (4.8)–(4.11) from (4.12) we easily obtain (4.13), which concludes the proof. □

5 Error estimate

Preliminaries. Given $k\geq 0$, on each primal element $T\in\mathcal{T}_h$, let $\Lambda_k^T : L^2(T)\to\mathcal{P}_k(T)$ denote the orthogonal L^2-projection operator, which satisfies the following approximation property (see, for instance, [18]): For all $s\in\{0,\ldots,k+1\}$, there holds

$$|v-\Lambda_k^T v|_{m,T} \leq Ch_T^{s-m}|v|_{s,T} \quad \forall v\in \mathrm{H}^m(T),\, \forall\, m\in\{0,\ldots,s\}. \tag{5.1}$$

We will also use a vector version of Λ_k^T, say $\boldsymbol{\Lambda}_k^T : \mathbf{L}^2(T)\to\mathbf{P}_k(T)$, which is defined component-wise by Λ_k^T. Then, we define the global operators $\boldsymbol{\Pi}_1 : \mathbf{H}(h)\to\mathbf{H}_h$ and $\Lambda_0 : \mathrm{Q}\to\mathrm{Q}_h$ by

$$(\boldsymbol{\Pi}_1\boldsymbol{v})|_T := \mathbf{P}_1^T\boldsymbol{v}, \quad (\Lambda_0 q)|_T := \Lambda_0^T q \quad \forall T\in\mathcal{T}_h.$$

It is clear that operator Λ_0 satisfies the approximation property

$$\|v-\Lambda_0 v\|_{0,\Omega} \leq Ch|v|_{1,T} \quad \forall v\in \mathrm{H}^1(\Omega). \tag{5.2}$$

In turn, from inequality (4.1) we observe that operator $\boldsymbol{\Pi}_1$ satisfies

$$\int_e \frac{1}{h_e}[\![\boldsymbol{u}-\boldsymbol{\Pi}_1\boldsymbol{u}]\!]^2 \leq C(h_e^{-2}|\boldsymbol{u}-\boldsymbol{\Pi}_1\boldsymbol{u}|_{0,T}^2 + |\boldsymbol{u}-\boldsymbol{\Pi}_1\boldsymbol{u}|_{1,T}^2). \tag{5.3}$$

We can then utilise the definition of the norm $|||\cdot|||_h$ together with estimates (5.1) with $m=1$ and $s=2$, and (5.3), to obtain the bound

$$|||\boldsymbol{u}-\boldsymbol{\Pi}_1\boldsymbol{u}|||_h \leq Ch\,|\boldsymbol{u}|_{2,\Omega}\,. \tag{5.4}$$

Let us now recall the Raviart-Thomas interpolation operator $\Pi_{\rm div} : \mathbf{H}^1(\Omega) \to \mathbf{Z}_h$, which, given $\boldsymbol{\tau} \in \mathbf{H}^1(\Omega)$, is characterised by the following identities:

$$\int_e (\Pi_{\rm div}(\boldsymbol{\tau}) \cdot \boldsymbol{n})\, r = \int_e (\boldsymbol{\tau} \cdot \boldsymbol{n}) r \qquad \forall\, e \in \mathcal{E}_h,\ \forall\, r \in P_0(e). \tag{5.5}$$

As a consequence of (5.5), there holds

$$\operatorname{div}(\Pi_{\rm div}(\boldsymbol{\tau})) = \Lambda_0(\operatorname{div} \boldsymbol{\tau}).$$

In addition, the operator $\Pi_{\rm div}$ satisfies the following approximation properties (see for instance [13]):

$$\|\boldsymbol{\tau} - \Pi_{\rm div}(\boldsymbol{\tau})\|_{0,T} \leq c_1 h_T |\boldsymbol{\tau}|_{1,T} \qquad \forall\ T \in \mathcal{T}_h, \tag{5.6}$$

for each $\boldsymbol{\tau} \in \mathbf{H}^1(\Omega)$, and

$$\|\operatorname{div}(\boldsymbol{\tau} - \Pi_{\rm div}(\boldsymbol{\tau}))\|_{0,T} \leq c_2 h_T |\operatorname{div} \boldsymbol{\tau}|_{1,T} \qquad \forall\ T \in \mathcal{T}_h, \tag{5.7}$$

for each $\boldsymbol{\tau} \in \mathbf{H}^1(\Omega)$, such that $\operatorname{div} \boldsymbol{\tau} \in \mathrm{H}^1(\Omega)$. Combining (5.6) and (5.7) it is clear that the following global estimate holds

$$\|\boldsymbol{\tau} - \Pi_{\rm div}(\boldsymbol{\tau})\|_{\operatorname{div},\Omega} \leq Ch(|\boldsymbol{\tau}|_{1,\Omega} + |\operatorname{div} \boldsymbol{\tau}|_{1,\Omega}), \tag{5.8}$$

for each $\boldsymbol{\tau} \in \mathbf{H}^1(\Omega)$, such that $\operatorname{div} \boldsymbol{\tau} \in \mathrm{H}^1(\Omega)$. After these preliminary steps we embark in proving optimal error estimates.

Theorem 5.1 *Let $(\boldsymbol{u}, \phi, \boldsymbol{\sigma}, p)$ and $(\boldsymbol{u}_h, \phi_h, \boldsymbol{\sigma}_h, p_h)$ be the solutions of (2.6)-(2.9) and (3.1)-(3.4), respectively, and let us assume that $\boldsymbol{u} \in \mathbf{H}^2(\Omega)$, $\boldsymbol{\sigma} \in \mathbf{H}^1(\Omega)$, $\operatorname{div} \boldsymbol{\sigma} \in \mathrm{H}^1(\Omega)$, and $\phi, p \in \mathrm{H}^1(\Omega)$. Then, there exists a constant $C > 0$ independent of both h and λ, such that*

$$\begin{aligned} &|||\boldsymbol{u} - \boldsymbol{u}_h|||_h + \|\phi - \phi_h\|_{0,\Omega} + \|\boldsymbol{\sigma} - \boldsymbol{\sigma}_h\|_{\operatorname{div},\Omega} + \|p - p_h\|_{0,\Omega} \\ &\qquad \leq Ch(\|\boldsymbol{u}\|_{2,\Omega} + \|\phi\|_{1,\Omega} + \|\boldsymbol{\sigma}\|_{1,\Omega} + \|\operatorname{div} \boldsymbol{\sigma}\|_{1,\Omega} + \|p\|_{1,\Omega}). \end{aligned}$$

Proof. Let $(\boldsymbol{u}, \phi, \boldsymbol{\sigma}, p)$ and $(\boldsymbol{u}_h, \phi_h, \boldsymbol{\sigma}_h, p_h)$ be the solutions of (2.6)-(2.9) and (3.1)-(3.4), respectively. To simplify the subsequent analysis, we write $\mathbf{e}_{\boldsymbol{u}} := \boldsymbol{u} - \boldsymbol{u}_h$, $e_\phi := \phi - \phi_h$, $\mathbf{e}_{\boldsymbol{\sigma}} := \boldsymbol{\sigma} - \boldsymbol{\sigma}_h$ and $e_p := p - p_h$. As usual, we shall then decompose these errors into

$$\mathbf{e}_{\boldsymbol{u}} = \boldsymbol{\xi}_{\boldsymbol{u}} + \boldsymbol{\chi}_{\boldsymbol{u}}, \quad e_\phi = \xi_\phi + \chi_\phi, \quad \mathbf{e}_{\boldsymbol{\sigma}} = \boldsymbol{\xi}_{\boldsymbol{\sigma}} + \boldsymbol{\chi}_{\boldsymbol{\sigma}} \quad \text{and} \quad e_p = \xi_p + \chi_p, \tag{5.9}$$

where

$$\begin{aligned} &\boldsymbol{\xi}_{\boldsymbol{u}} := \boldsymbol{u} - \boldsymbol{\Pi}_1(\boldsymbol{u}), \quad \boldsymbol{\chi}_{\boldsymbol{u}} := \boldsymbol{\Pi}_1(\boldsymbol{u}) - \boldsymbol{u}_h, \quad \xi_\phi := \phi - \Lambda_0(\phi), \quad \chi_\phi := \Lambda_0(\phi) - \phi_h, \\ &\boldsymbol{\xi}_{\boldsymbol{\sigma}} := \boldsymbol{\sigma} - \boldsymbol{\Pi}_{\rm div}(\boldsymbol{\sigma}) \quad \boldsymbol{\chi}_{\boldsymbol{\sigma}} := \boldsymbol{\Pi}_{\rm div}(\boldsymbol{\sigma}) - \boldsymbol{\sigma}_h \quad \xi_p := p - \Lambda_0(p), \quad \chi_p := \Lambda_0(p) - p_h. \end{aligned}$$

Then, in what follows we prove that there exists $C > 0$, independent of h and λ, such that

$$|||\boldsymbol{\chi}_{\boldsymbol{u}}|||_h + \|\chi_\phi\|_{0,\Omega} + \|\boldsymbol{\chi}_{\boldsymbol{\sigma}}\|_{\operatorname{div},\Omega} + \|\chi_p\|_{0,\Omega} \leq C(|||\boldsymbol{\xi}_{\boldsymbol{u}}|||_h + \|\xi_\phi\|_{0,\Omega} + \|\boldsymbol{\xi}_{\boldsymbol{\sigma}}\|_{\operatorname{div},\Omega} + \|\xi_p\|_{0,\Omega}),$$

thus the desired result can be easily obtained from the latter, the triangle inequality and estimates (5.2), (5.4) and (5.8). We begin by noticing that since we assume $\boldsymbol{u} \in \mathbf{H}^2(\Omega)$, then for all $\boldsymbol{v}_h \in \mathbf{H}_h$ there hold $a_s^h(\boldsymbol{u}, \boldsymbol{v}_h) = a_s(\boldsymbol{u}, \boldsymbol{v}_h)$ and $b_s^h(\boldsymbol{u}, \psi_h) = \tilde{b}_s^h(\boldsymbol{u}, \psi_h) = b_s(\boldsymbol{u}, \psi_h)$. In this way, restricting the test functions in (2.6)–(2.9) to the corresponding finite dimensional spaces, and subtracting the resulting set of equations with (3.1)–(3.4), we easily obtain the Galerkin orthogonality property

$$\begin{aligned} a_s^h(\mathbf{e}_{\boldsymbol{u}}, \boldsymbol{v}_h) + b_s^h(\boldsymbol{v}_h, e_\phi) &= 0 \quad \forall \boldsymbol{v}_h \in \mathbf{H}_h, \\ \tilde{b}_s^h(\mathbf{e}_{\boldsymbol{u}}, \psi_h) - c_s(e_\phi, \psi_h) + b_{sf}(\psi_h, e_p) &= 0 \quad \forall \psi_h \in \mathrm{Q}_h, \end{aligned}$$

$$
\begin{aligned}
a_f(\mathbf{e}_{\boldsymbol{\sigma}}, \boldsymbol{\tau}_h) + b_f(\boldsymbol{\tau}_h, e_p) &= 0 \quad \forall \boldsymbol{\tau}_h \in \mathbf{Z}_h, \\
b_{sf}(e_\phi, q_h) + b_f(\mathbf{e}_{\boldsymbol{\sigma}}, q_h) - c_f(e_p, q_h) &= 0 \quad \forall q_h \in \mathrm{Q}_h,
\end{aligned}
$$

which, together with the decompositions (5.9), implies that

$$
\begin{aligned}
a_s^h(\boldsymbol{\chi}_{\boldsymbol{u}}, \boldsymbol{v}_h) + b_s^h(\boldsymbol{v}_h, \chi_\phi) &= F_1^h(\boldsymbol{v}_h) \quad \forall \boldsymbol{v}_h \in \mathbf{H}_h, \\
\tilde{b}_s^h(\boldsymbol{\chi}_{\boldsymbol{u}}, \psi_h) - c_s(\chi_\phi, \psi_h) + b_{sf}(\psi_h, \chi_p) &= G_1^h(\psi_h) \quad \forall \psi_h \in \mathrm{Q}_h, \\
a_f(\boldsymbol{\chi}_{\boldsymbol{\sigma}}, \boldsymbol{\tau}_h) + b_f(\boldsymbol{\tau}_h, \chi_p) &= F_2^h(\boldsymbol{\tau}_h) \quad \forall \boldsymbol{\tau}_h \in \mathbf{Z}_h, \\
b_{sf}(\chi_\phi, q_h) + b_f(\boldsymbol{\chi}_{\boldsymbol{\sigma}}, q_h) - c_f(\chi_p, q_h) &= G_2^h(q_h) \quad \forall q_h \in \mathrm{Q}_h,
\end{aligned}
\tag{5.10}
$$

with

$$
\begin{aligned}
F_1^h(\boldsymbol{v}_h) &:= -a_s^h(\boldsymbol{\xi}_{\boldsymbol{u}}, \boldsymbol{v}_h) - b_s^h(\boldsymbol{v}_h, \xi_\phi), \quad G_1^h(\psi_h) := c_s(\xi_\phi, \psi_h) - \tilde{b}_s^h(\boldsymbol{\xi}_{\boldsymbol{u}}, \psi_h) - b_{sf}(\psi_h, \xi_p), \\
F_2^h(\boldsymbol{\tau}_h) &:= -a_f(\boldsymbol{\xi}_{\boldsymbol{\sigma}}, \boldsymbol{\tau}_h) - b_f(\boldsymbol{\tau}_h, \xi_p), \quad G_2^h(q_h) := c_f(\xi_p, q_h) - b_{sf}(\xi_\phi, q_h) - b_f(\boldsymbol{\xi}_{\boldsymbol{\sigma}}, q_h).
\end{aligned}
$$

Then, applying Theorem 4.1 to (5.10) we deduce that there exists $C > 0$, independent of λ and h, such that

$$
|||\boldsymbol{\chi}_{\boldsymbol{u}}|||_h + \|\chi_\phi\|_{0,\Omega} + \|\boldsymbol{\chi}_{\boldsymbol{\sigma}}\|_{\mathrm{div},\Omega} + \|\chi_p\|_{0,\Omega} \leq C(\|F_1^h\|_{\mathbf{H}_h'} + \|G_1^h\|_{\mathrm{Q}_h'} + \|F_2^h\|_{\mathbf{Z}_h'} + \|G_2^h\|_{\mathrm{Q}_h'}). \tag{5.11}
$$

Now we proceed to bound the norms on the right-hand side of (5.11). We start by observing that from the continuity of a_s^h and b_s^h (cf.(4.2) and (4.7), respectively), we obtain

$$
\|F_1^h\|_{\mathbf{H}_h'} \leq c_1(|||\boldsymbol{\xi}_{\boldsymbol{u}}|||_h + \|\xi_\phi\|_{0,\Omega}),
$$

with $c_1 > 0$ independent of λ and h. In turn, using again the continuity of b_s^h, together to the continuity of c_s and b_{sf} (cf. (2.11)), it follows that

$$
\|G_1^h\|_{\mathrm{Q}_h'} \leq c_2(\lambda^{-1}\|\xi_\phi\|_{0,\Omega} + \lambda^{-1}\|\xi_p\|_{0,\Omega} + |||\boldsymbol{\xi}_{\boldsymbol{u}}|||_h),
$$

with $c_2 > 0$ independent of λ and h. Next, to bound $\|F_2^h\|_{\mathbf{Z}_h'}$ we make us of the continuity of a_f and b_f (cf. (2.11)) to get

$$
\|F_2^h\|_{\mathbf{Z}_h'} \leq c_3(\|\boldsymbol{\xi}_{\boldsymbol{\sigma}}\|_{\mathrm{div},\Omega} + \|\xi_p\|_{0,\Omega}),
$$

with $c_3 > 0$ independent of λ and h. Finally, the continuity of c_f, b_{sf} and b_f (cf. (2.11)) imply

$$
\|G_2^h\|_{\mathrm{Q}_h'} \leq c_4(\|\xi_p\|_{0,\Omega} + \lambda^{-1}\|\xi_\phi\|_{0,\Omega} + \|\boldsymbol{\xi}_{\boldsymbol{\sigma}}\|_{\mathrm{div},\Omega}), \tag{5.12}
$$

with $c_4 > 0$ independent of λ and h. Therefore, from (5.11)–(5.12) we obtain that there exists $C > 0$, independent of λ and h, such that

$$
|||\boldsymbol{\chi}_{\boldsymbol{u}}|||_h + \|\chi_\phi\|_{0,\Omega} + \|\boldsymbol{\chi}_{\boldsymbol{\sigma}}\|_{\mathrm{div},\Omega} + \|\chi_p\|_{0,\Omega} \leq C(|||\boldsymbol{\xi}_{\boldsymbol{u}}|||_h + (1+2\lambda^{-1})\|\xi_\phi\|_{0,\Omega} + \|\boldsymbol{\xi}_{\boldsymbol{\sigma}}\|_{\mathrm{div},\Omega} + (2+\lambda^{-1})\|\xi_p\|_{0,\Omega}),
$$

which together to the fact that $1 + 2\lambda^{-1}$ and $2 + \lambda^{-1}$ can be seen as constants independent of λ if $\lambda \to \infty$, concludes the proof. □

6 Numerical verification

We now provide a set of examples serving to illustrate convergence and locking-free properties of the proposed method. In contrast with the computational implementation of conforming FVE schemes (where only mass and source terms need to define matrix blocks that interact with the control volumes in the dual meshes), our coupled DFV-MFE solver uses an explicit construction of the inter-mesh projection map, as the associated interpolation matrix is used in the contributions due to strain and

DoF	h	$\|\boldsymbol{u}-\boldsymbol{u}_h\|_{0,\Omega}$		$\|\!\|\!\|\boldsymbol{u}-\boldsymbol{u}_h\|\!\|\!\|_h$		$\|\phi-\phi_h\|_{0,\Omega}$		$\|\boldsymbol{\sigma}-\boldsymbol{\sigma}_h\|_{0,\Omega}$		$\|\boldsymbol{\sigma}-\boldsymbol{\sigma}_h\|_{\mathrm{div},\Omega}$		$\|p-p_h\|_{0,\Omega}$	
		error	rate	error	rate	error	rate	error	rate	error	rate	error	rate
$\nu = 0.4$													
80	0.7810	0.0744	–	0.6926	–	3.6644	–	1.2167	–	2.3256	–	0.3773	–
177	0.5207	0.0619	0.45	0.5504	0.57	2.2433	0.69	0.9013	0.74	1.6331	0.87	0.2476	1.04
485	0.3124	0.0331	1.22	0.4091	0.58	1.1622	0.84	0.5755	0.88	0.9954	0.97	0.1456	1.04
1557	0.1736	0.0133	1.55	0.2559	0.79	0.5785	0.94	0.3296	0.94	0.5581	0.98	0.0799	1.02
5525	0.0919	0.0042	1.80	0.1409	0.94	0.3190	0.75	0.1767	0.98	0.2967	0.99	0.0421	1.01
20757	0.0473	0.0012	1.95	0.0734	0.98	0.1665	0.94	0.0914	0.99	0.1531	0.99	0.0217	1.00
80405	0.0240	0.0003	1.98	0.0374	0.99	0.0842	1.00	0.0465	0.99	0.0778	1.00	0.0110	1.00
316437	0.0121	0.0001	1.99	0.0189	1.00	0.0422	1.00	0.0234	1.00	0.0392	1.00	0.0055	1.00
$\nu = 0.495$													
80	0.7810	0.0834	–	0.6878	–	5.3694	–	1.2179	–	2.3261	–	0.3774	–
177	0.5207	0.0832	0.42	0.5843	0.50	2.4471	0.90	0.9020	0.75	1.6322	0.87	0.2479	1.03
485	0.3124	0.0466	1.53	0.4534	0.59	1.6185	0.64	0.5756	0.87	0.9938	0.97	0.1456	1.04
1557	0.1736	0.0191	1.61	0.2892	0.76	1.0467	0.65	0.3296	0.94	0.5568	0.98	0.0799	1.02
5525	0.0919	0.0062	1.77	0.1606	0.92	0.6353	0.79	0.1767	0.98	0.2959	0.99	0.0421	1.01
20757	0.0473	0.0017	1.96	0.0836	0.98	0.3675	0.83	0.0914	0.99	0.1526	0.99	0.0217	1.00
80405	0.0240	0.0004	2.05	0.0424	1.00	0.1955	0.93	0.0465	0.99	0.0775	1.00	0.0110	1.00
316437	0.0121	0.0001	1.94	0.0213	1.00	0.1051	0.95	0.0234	0.99	0.0391	1.00	0.0055	1.00
$\nu = 0.49999$													
80	0.7810	0.1243	–	0.6877	–	6.9456	–	1.2180	–	2.3262	–	0.3774	–
177	0.5207	0.0855	0.33	0.5884	0.39	4.8192	0.84	0.9021	0.74	1.6323	0.87	0.2479	1.03
485	0.3124	0.0480	1.12	0.4584	0.48	2.7653	0.93	0.5756	0.88	0.9938	0.97	0.1456	1.04
1557	0.1736	0.0198	1.51	0.2928	0.76	1.7567	0.92	0.3296	0.95	0.5568	0.98	0.0799	1.02
5525	0.0919	0.0065	1.74	0.1630	0.92	0.9291	0.75	0.1767	0.98	0.2959	0.99	0.0421	1.00
20757	0.0473	0.0019	1.91	0.0851	0.98	0.4892	0.86	0.0914	0.99	0.1526	0.99	0.0217	1.00
80405	0.0240	0.0005	2.01	0.0433	0.99	0.2657	0.86	0.0465	0.99	0.0775	1.00	0.0110	1.00
316437	0.0121	0.0001	2.01	0.0218	1.00	0.1632	0.74	0.0234	1.00	0.0391	1.00	0.0055	1.00

Table 1: Test 1. Error history for the DFV-MFE scheme (3.1)-(3.4) approximating the four-field poroelasticity equations for different value of the elasticity parameters.

the off-diagonal bilinear forms $b_1^h(\cdot,\cdot)$ and $\tilde{b}_1^h(\cdot,\cdot)$. All operations involving matrix assembly and the solution of linear systems using distributed Krylov solvers, were performed with an in-house code based on the libraries Trilinos (www.trilinos.org) and OpenMPI (www.open-mpi.org), and primal meshes were generated with GMSH [14].

Example 1: convergence test and locking. In order to experimentally confirm the error estimates derived in Theorem 5.1 we consider a rectangular domain $\Omega = (0, 3/2) \times (0, 1)$, where the boundaries are split as $\Gamma_{\boldsymbol{u}} = \{(x, y) : x = 0 \text{ or } y = 1\}$ and $\Gamma_p = \{(x, y) : x = 3/2 \text{ or } y = 0\}$. We employ the approach of manufactured solutions and propose the following closed form solutions to (2.1)-(2.4)

$$\boldsymbol{u} = \begin{pmatrix} -16x^2(x-1)^2y(y-1)(2y-1) + \frac{x^2}{2E\lambda} \\ 16y^2(y-1)^2x(x-1)(2x-1) + \frac{y^2}{2E\lambda} \end{pmatrix}, \; p = x^3 - y^4, \; \phi = p - \lambda \operatorname{div} \boldsymbol{u}, \; \boldsymbol{\sigma} = -\frac{\kappa}{\eta}(\nabla p - \rho \boldsymbol{g}).$$

These smooth functions are used to construct a body force $\boldsymbol{f}$, a fluid source ℓ, the non-homogeneous Dirichlet pressure p_Γ, and a non-homogeneous normal stress defined on Γ_p. The non-dimensional model and discretisation parameters adopted in this test are chosen as follows: $\eta = c_0 = \kappa_0 = 0.001$, $\alpha = \rho = \theta = 1$, $\kappa(\boldsymbol{x}) = \kappa_0[1 + \kappa_0 \sin^2(\pi x)\cos^2(\pi y)]$, $\boldsymbol{g} = (0, -1)^T$, $\gamma_{\boldsymbol{u}} = 1000$, and $\gamma_\phi = 0.1$. The

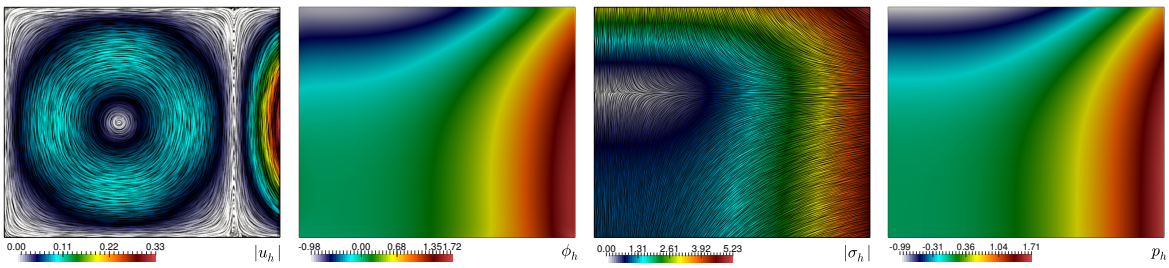

(a) (b) (c) (d)

Figure 2: Test 1. Approximate displacement magnitude (a), total pressure (b), fluid flux (c), and fluid pressure (c); computed for $\mu = 33.44$, $\lambda = 3311.04$, on a mesh with 33282 primal elements.

Young modulus is $E = 100$, whereas for the Poisson ratio we will consider three cases assigning $\nu = 0.4$ (giving $\mu = 35.71$, $\lambda = 42.857$) $\nu = 0.495$ (with $\mu = 33.44$, $\lambda = 3311.04$), and $\nu = 0.4999$ (implying $\mu = 33.333$, $\lambda = 1.666\text{e}4$).

On a sequence of uniformly refined meshes we produce approximate solutions using the proposed DFV-MFE method, and in Table 1 we collect errors computed in the norms suggested by the analysis of Section 5, together with convergence rates calculated as

$$\texttt{rate} = \log\left(\frac{e(\cdot)}{\widehat{e}(\cdot)}\right)[\log(h/\widehat{h})]^{-1},$$

where $e, \widehat{e}$ stand for errors generated by methods defined on meshes with meshsizes $h, \widehat{h}$, respectively. We can see that the error decay provides verification of the overall first order approximation anticipated by our theoretical results, holding irrespectively of the value of λ. The converged solutions for the intermediate value of the Poisson ratio, are displayed in Figure 2. The linear solves were performed using the BiCGStab method.

Example 2: surface footing. We next address the numerical solution of a partial compression problem in 3D. One seeks to determine the deformation as well as the undrained response of the fluid (flux and pressure distribution) of a porous material when subject to a distributed boundary load of magnitude 10000. The computational domain occupied by the porous medium is a box whose left, right, back and front faces are defined by $x = -100, x = 100, y = 100, y = -100$, while the top and bottom surfaces are defined by the parameterisation

$$t \mapsto z(x, y, t) = 12\cos(0.01[x + \pi y])\cos^2(0.01[\pi x + y]) + \frac{1}{4}t + \frac{1}{12}(0.01y - 1), \quad t \in [-100, 100],$$

(see e.g. [16]). Its boundary is separated into $\Omega_{\Gamma_{\boldsymbol{u}}}$ and Ω_{Γ_p}. The former contains portions of the boundary corresponding to the faces $y = -100$, $y = 100$ and $x = 100$, where we will prescribe zero displacements $\boldsymbol{u} = \boldsymbol{0}$ and zero normal fluid flux $\sigma \cdot \boldsymbol{n} = 0$. On the remainder of $\partial\Omega$ we set zero fluid pressure $p_\Gamma = 0$, and assume a non-homogeneous total normal stress

$$\boldsymbol{h}_\Gamma = \begin{cases} (10000, 0, 0)^T & \text{if } x = -100 \text{ and } -50 \leq y \leq 50, \\ 0 & \text{otherwise,} \end{cases}$$

imposed according to the condition $(2\mu\boldsymbol{\varepsilon}(\boldsymbol{u}) - \phi\mathbf{I}) = \boldsymbol{h}_\Gamma$, on Ω_{Γ_p}. In addition we consider a null source $\boldsymbol{f} = \boldsymbol{0}$, a constant fluid source $\ell = 0.01$, the gravity force $\boldsymbol{g} = (0, 0, -9.8)^T$, Young and Poisson elastic moduli $E = 30000$, $\nu = 0.475$, storage and Biot-Willis coefficients $c_0 = 0.001$, $\alpha = 0.1$, permeability of the porous matrix $\kappa = 0.0001$, fluid viscosity $\eta = 0.01$, and fluid density $\rho = 500$. The primal mesh

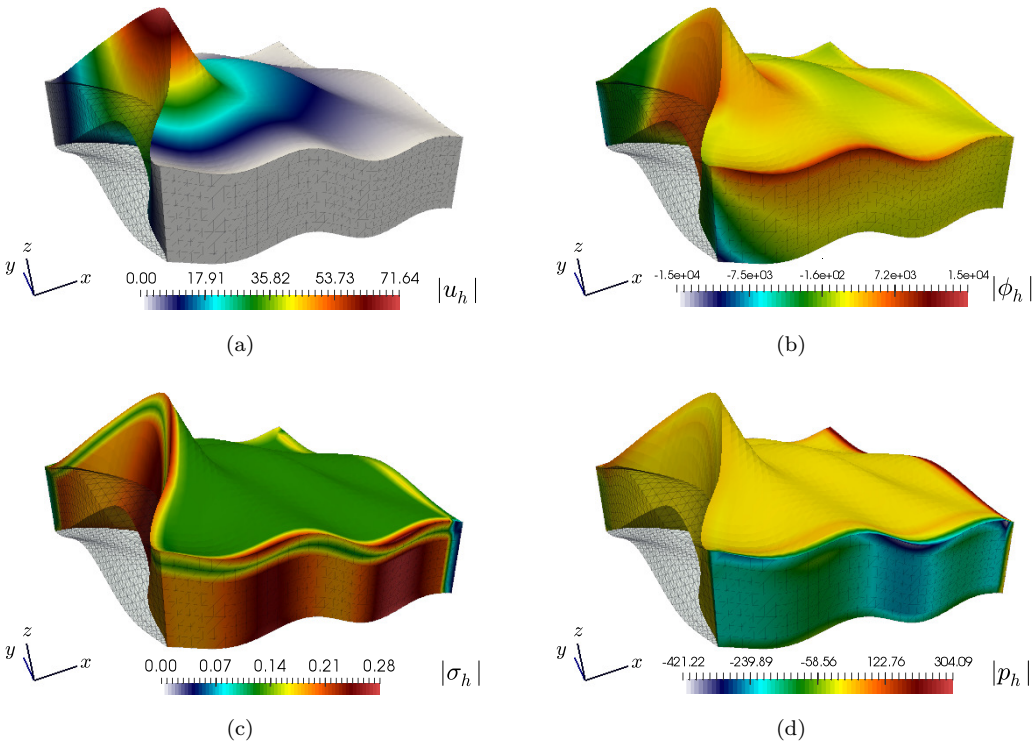

Figure 3: Test 2. Deformation and filtration response of a porous block subjected to a normal boundary force at one end. Displacement magnitude (a), total pressure distribution (b), fluid flux (c), and fluid pressure (d).

contains 49152 tetrahedral elements and we take the penalisation parameters $\gamma_{\boldsymbol{u}} = 100$, $\gamma_\phi = 1e-5$, together with the symmetric version of the interior penalty method (i.e. $\theta = 1$).

The obtained approximate solutions are depicted in Figure 3, and rendered on the deformed domain. We also show the undeformed skeleton mesh in each panel. For this test (as well as for test 4 below) we have used a GMRES solver with a tolerance of 1e-6, and preconditioned by an ILU factorisation.

Example 3: loading of a cylindrical shell. For this test we study a transient problem where (2.4) adopts the form

$$\frac{\partial}{\partial t}\left[\left(c_0 + \frac{\alpha}{\lambda}\right)p - \frac{\alpha}{\lambda}\phi\right] + \operatorname{div}\boldsymbol{\sigma} = \ell \quad \text{in } \Omega \times (0, T_{\text{final}}), \tag{6.1}$$

where $t \in (0, T)$ denotes the time variable and $T_{\text{final}} > 0$ is a given final time. As in [1] we consider a 2D domain (a ring of external radius 1 and internal radius 0.5) representing the cross-section of a cylindrical shell made of a deformable porous material. The outer circle will be considered as $\Gamma_{\boldsymbol{u}}$ so we impose the domain to be clamped and the normal flux of the fluid pressure is zero. On the inner circle, Γ_p, we impose a fixed fluid pressure $p_\Gamma = 1$ and an *effective solid stress*

$$[2\mu\boldsymbol{\varepsilon}(\boldsymbol{u}) + \lambda(\operatorname{div}\boldsymbol{u})\mathbf{I}]\boldsymbol{n} = -(\cos(\theta), \sin(\theta))^T,$$

where θ is the second polar coordinate. This implies that the total traction load to impose at Γ_p is $-(\cos(\theta), \sin(\theta)) - p_\Gamma$. We assume the absence of gravitational forces, $\boldsymbol{g} = \mathbf{0}$, and we take a zero specific storage $c_0 = 0$. Such a configuration is of particular importance as low values of the specific storage have been reported to induce volumetric locking. As we will observe below, the proposed

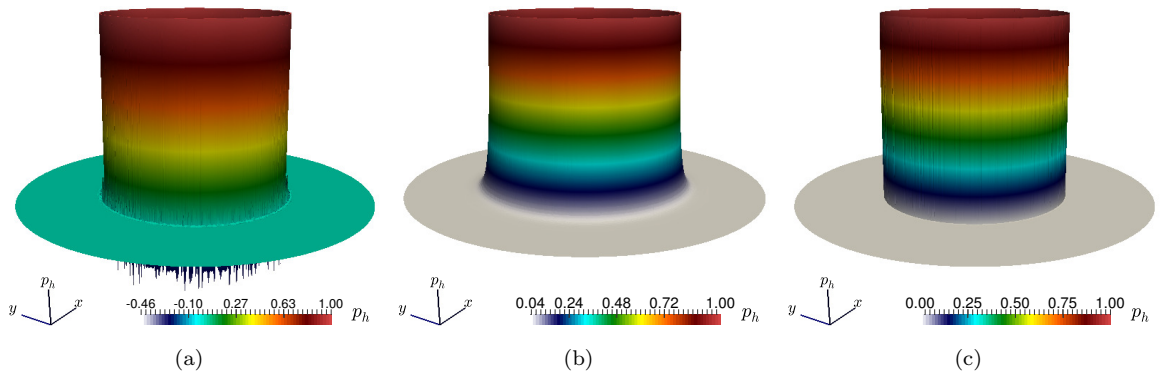

(a) (b) (c)

Figure 4: Test 3. Transient loading of a cylindrical shell. Elevation plots according to the fluid pressure computed with: a primal conforming piecewise linear approximation of solid displacement and pressure (a), adding a model stabilisation $-\beta\Delta\left[\frac{\partial}{\partial t}p\right]$ with $\beta = h^2/(4\lambda + 8\mu)$ (b), and with the proposed mixed-mixed formulation (c).

mixed-mixed formulation seems to completely remove any issues associated to $c_0 = 0$. The remaining model parameters take on the following values $E = 10000$, $\nu = 0.2$, $\alpha = 1$, $\kappa = 1e-7$, $\eta = 1e-3$. The primal mesh contains 37084 triangular elements, and the time discretisation of the problem follows a classical backward Euler scheme with a fixed timestep $\Delta t = 1e-6$. The stabilisation constants are set as $\gamma_{\boldsymbol{u}} = 10$, $\gamma_\phi = 0.1$ and again we adopt a symmetric interior penalty method.

The model and methods in [1] suggest to incorporate a stabilisation term $-\beta\Delta\left[\frac{\partial}{\partial t}p\right]$ on the left hand side of (6.1), with $\beta > 0$ depending on the Lamé constants and the meshsize. We perform a comparison against a conforming discretisation of the Biot consolidation problem formulated solely in terms of solid displacement and fluid pressure, using piecewise linear and continuous Lagrange finite elements for $\boldsymbol{u}$ and p, and incorporating $\beta = h^2/(4\lambda + 8\mu)$. We observe that such a stabilisation (targeted to eliminate oscillations near the inner boundary Γ_p) generates a marked smoothing of the fluid pressure profile, which is not necessarily consistent with the expected physical behaviour. We also mention that this stabilisation is actually not required in our mixed-mixed method, due to the conservative character of the scheme and its suitability for handling discontinuities and high gradients. The obtained results are displayed in Figure 4.

Example 4: two-layered porous material. We now simulate the drainage behaviour of a porous region composed of two layers with different material properties determined by the discontinuous Lamé moduli of dilation and shear, and the solid permeability

$$\lambda = \mu = \begin{cases} 1e4 & \text{in } \Omega_{\text{bot}}, \\ 1 & \text{in } \Omega_{\text{top}}, \end{cases}, \quad \kappa = \begin{cases} 0.1 & \text{in } \Omega_{\text{bot}}, \\ 1e-4 & \text{in } \Omega_{\text{top}}, \end{cases}$$

where $\Omega = (0,1)^3 = \Omega_{\text{bot}} \cup \Omega_{\text{top}}$ with the two subdomains being separated by the plane $z = 0.5$. The solid matrix in the upper domain is softer and less permeable than the material occupying the bottom layer (see a similar test performed in [24]). The constants dictating the hydromechanical coupling (that is, the specific storage and Biot-Willis parameter) are specified as $c_0 = 0.009, \alpha = 1$, and the remaining data are $\eta = 1$, $\gamma_{\boldsymbol{u}} = 100$, $\gamma_\phi = 0.01$.

As in Example 2 above, the onset of motion and flow is induced by applying a normal surface load on a part of the boundary. We now use a load of magnitude 5 applied on a disk of centre $(1/4, 1/4, 1)$ and radius 0.2, lying on the top lid. The remainder of the top face, together with the whole bottom square and the faces $x = 0$ and $y = 0$ constitute Γ_p (where the fluid pressure is set to zero and the fluid content is free to drain), whereas we assume that the two remaining lateral walls, defined by

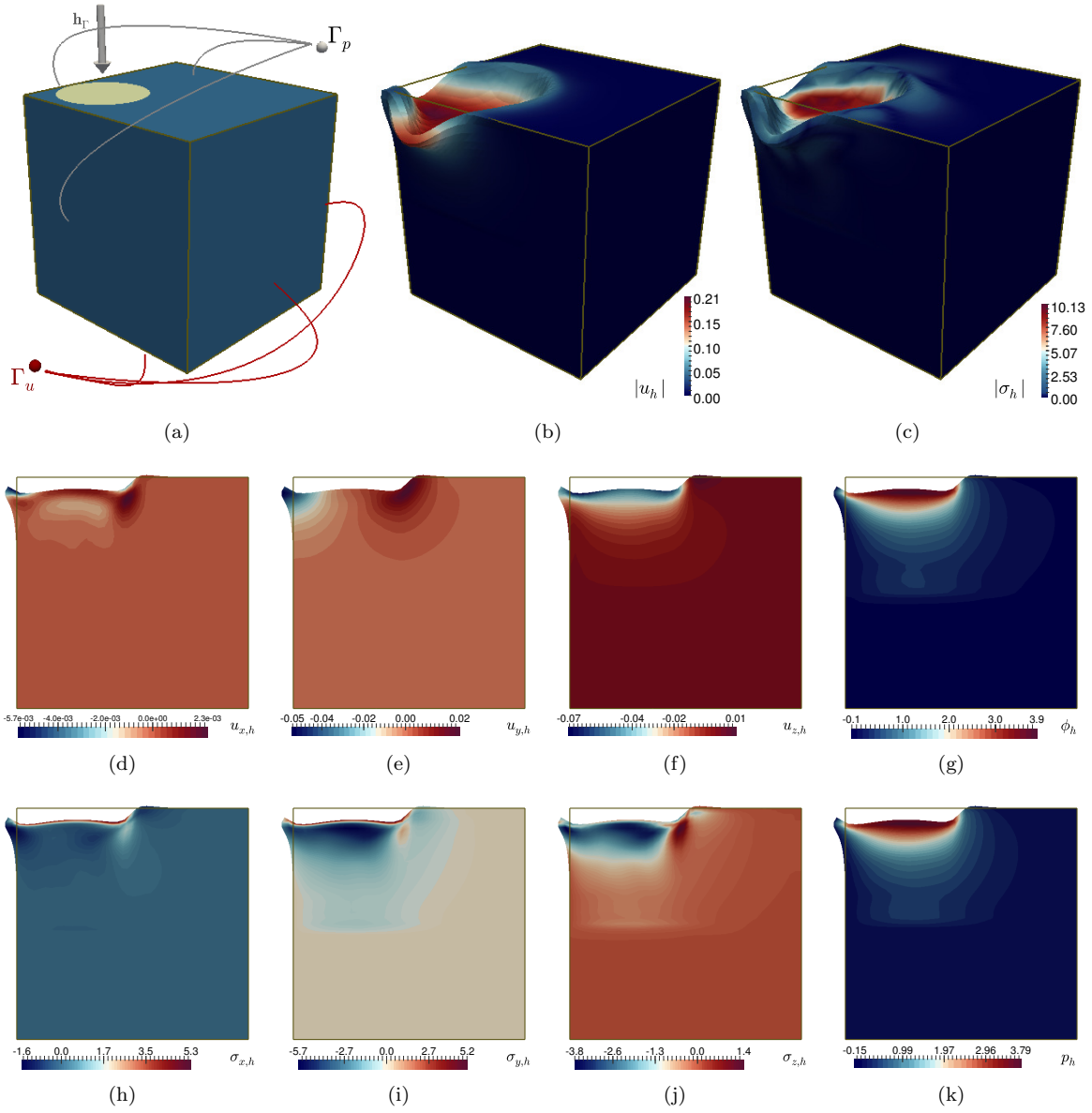

Figure 5: Test 4. Deformation and filtration response of a two-layered medium. Sketch of the domain configuration and boundary conditions (a), displacement magnitude (b), fluid flux (c); and snapshots of each scalar field on the slice $x = 0.25$ (d-k).

$x = 1$ and $y = 1$, are completely rigid and impermeable (on this boundary part, $\Gamma_{\boldsymbol{u}}$, we impose zero displacements and zero normal fluid flux). The domain configuration and the boundary labels are sketched in Figure 6. We took a uniform mesh having 345'600 tetrahedral elements in the primal mesh, resulting in a linear system of 5'538'560 unknowns.

Snapshots of the solutions computed using the proposed DFV-MFE scheme are shown in Figure 5, exhibiting a qualitative agreement with the results from [24]. In particular, the produced approximations do not present spurious oscillations in the computed total and fluid pressures, nor unphysically small displacements. We can also observe that the pressure distributions form an interior boundary layer, but these high gradients do not pollute the numerical approximation.

Summary and concluding remarks. We have introduced a new mixed-mixed formulation for linear elasticity using the total pressure and the fluid flux as additional mixed variables. The proposed discretisation consisted on a combined discontinuous finite volume scheme for the displacement of the solid skeleton, and a mixed finite element method approximating the remaining fields. The method features conservativity, absence of spurious pressure oscillations, and locking free properties. We have derived theoretical error estimates and have confirmed them experimentally through a series of numerical tests in 2D and 3D.

As extensions of this work we foresee the development of suitable preconditioners and high-order discretisations for displacements and total pressure. A further step would be to derive a posteriori error estimates, focusing on the zones of fluid singularities and stress concentration [27]. We would also like to investigate fractures and energy conservation aspects as recently addressed in [7], as well as the generalisation of our theoretical and computational framework (presently confined to the linear case) to the study of interface problems in the regime of finite strains. We finally mention that large scale problems will require the design of suitable preconditioners, for which we can appeal to the recent developments in e.g. [19].

References

[1] Aguilar, F. Gaspar, F. Lisbona, and C. Rodrigo, *Numerical stabilization of Biot's consolidation model by a perturbation on the flow equation*. Int. J. Numer. Methods Engrg. **75** (2008) 1282–1300.

[2] D.N. Arnold, *An interior penalty finite element method with discontinuous elements*. SIAM J. Numer. Anal. **19** (1982) 742–760.

[3] R. Asadi, B. Ataie-Ashtiani, and C.T. Simmons, *Finite volume coupling strategies for the solution of a Biot consolidation model*. Comput. Geotech. **55** (2014) 494–505.

[4] L. Berger, R. Bordas, D. Kay, and S. Tavener, *Stabilized lowest-order finite element approximation for linear three-field poroelasticity*. SIAM J. Sci. Comput. **37** (2015) A2222–A2245.

[5] M.A. Biot, *Theory of elasticity and consolidation for a porous anisotropic solid*. J. Appl. Phys. **26** (1955) 182–185.

[6] D. Boffi, F. Brezzi and M. Fortin, Mixed Finite Element Methods and Applications. Springer Series in Computational Mathematics, 44. Springer, (2010)

[7] M. Bukač, I. Yotov, and P. Zunino, *Dimensional model reduction for flow through fractures in poroelastic media*. ESAIM: M2AN **51**(4) (2017) 1429–1471.

[8] C. Carstensen, N. Nataraj, and A.K. Pani, *Comparison results and unified analysis for first-order finite volume element methods for a Poisson model problem*. IMA J. Numer. Anal. **36**(3) (2016) 1120–1142.

[9] Y. Chen, Y. Luo, and M. Feng, *Analysis of a discontinuous Galerkin method for the Biot's consolidation problem*. Appl. Math. Comput. **219** (2013) 9043–9056.

[10] Q. Deng, V. Ginting, B. McCaskill, and P. Torsu, *A locally conservative stabilized continuous Galerkin finite element method for two-phase flow in poroelastic subsurfaces*. J. Comput. Phys. **347** (2017) 78–98.

[11] D. Di Pietro and A. Ern, Mathematical Aspects of Discontinuous Galerkin Methods. Mathématiques & Applications, 69. Springer, Heidelberg, (2012).

[12] X. Feng, Z. Ge, and Y. Li, *Analysis of a multiphysics finite element method for a poroelasticity model*. IMA J. Numer. Anal. **38**(1) (2018) 330–359.

[13] G.N. Gatica, *A Simple Introduction to the Mixed Finite Element Method. Theory and Applications*, Springer Briefs in Mathematics, Springer, Cham, (2014).

[14] C. Geuzaine and J.-F. Remacle, *Gmsh: a three-dimensional finite element mesh generator with built-in pre- and post-processing facilities*. Int. J. Numer. Methods Engrg. **79**(11) (2009) 1309–1331.

[15] V. Girault and P.-A. Raviart, Finite Element Approximation of the Navier–Stokes Equations. Lecture Notes in Mathematics, 749. Springer-Verlag, Berlin-New York, (1979).

[16] V. Girault, M.F. Wheeler, B. Ganis, and M.E. Mear, *A lubrication fracture model in a poro-elastic medium*. Math. Models Methods Appl. Sci. **25** (2015) 587–645.

[17] S. Kumar and R. Ruiz-Baier, *Equal order discontinuous finite volume element methods for the Stokes problem*. J. Sci. Comput. **65** (2015) 956–978.

[18] R. Lazarov and X. Ye, *Stabilized discontinuous finite element approximations for Stokes equations*. J. Comput. Appl. Math. **198**(1) (2007) 236–252.

[19] J.J. Lee, K.-A. Mardal, and R. Winther, *Parameter-robust discretization and preconditioning of Biot's consolidation model*. SIAM J. Sci. Comp. **39** (2017) A1–A24.

[20] R.W. Lewis and B.A. Schrefler, *The finite element method in the deformation of and consolidation of porous media*. Wiley & Sons, Chichester (1987).

[21] R. Liu, M.F. Wheeler, C.N. Dawson, and R.H. Dean, *On a coupled discontinuous/continuous Galerkin framework and an adaptive penalty scheme for poroelasticity problems*. Comput. Methods Appl. Mech. Engrg. **198** (2009) 3499–3510.

[22] M.A. Murad, V. Thomée, and A.F.D. Loula, *Asymptotic behavior of semi discrete finite-element approximations of Biot's consolidation problem*. SIAM J. Numer. Anal. **33** (1996) 1065–1083.

[23] A. Naumovich, *On finite volume discretization of the three-dimensional Biot poroelasticity system in multilayer domains*. Comput. Methods Appl. Math. **6** (2006) 306–325.

[24] A. Naumovich and F.J. Gaspar, *On a multigrid solver for the three-dimensional Biot poroelasticity system in multilayered domains*. Comput. Vis. Sci. **11** (2008) 77–87.

[25] R. Oyarzúa and R. Ruiz-Baier, *Locking-free finite element methods for poroelasticity*. SIAM J. Numer. Anal. **54**(5) (2016) 2951–2973.

[26] P.J. Phillips, and M.F. Wheeler, *A coupling of mixed and discontinuous Galerkin finite-element methods for poroelasticity*. Comput Geosci. **12** (2008) 417–435.

[27] R. Riedlbeck, D.A. Di Pietro, A. Ern, S. Granet, and K. Kazymyrenko, *Stress and flux reconstruction in Biot's poro-elasticity problem with application to a posteriori error analysis*. Comput. Math. Appl. **73** (2017) 1593–1610.

[28] B. Rivière, J. Tan, and T. Thompson, *Error analysis of primal discontinuous Galerkin methods for a mixed formulation of the Biot equations*. Comput. Math. Appl. **73** (2017) 666–683.

[29] R. Ruiz-Baier and I. Lunati, *Mixed finite element – discontinuous finite volume element discretization of a general class of multicontinuum models*. J. Comput. Phys. **322** (2016) 666–688.

[30] M. Sun and H. Rui, *A coupling of weak Galerkin and mixed finite element methods for poroelasticity*. Comput. Math. Appl. **73** (2017) 804–823.

[31] M.F. Wheeler, G. Xue, and I. Yotov, *Coupling multipoint flux mixed finite element methods with continuous Galerkin methods for poroelasticity*. Comput. Geosci. **18** (2014) 57–75.

[32] J. A. White and R.I. Borja, *Stabilized low-order finite elements for coupled solid-deformation/fluid-diffusion and their application to fault zone transients*. Comput. Methods Appl. Mech. Engrg. **197** (2008) 4353–4366.

[33] X. Ye, *A discontinuous finite volume method for the Stokes problem*. SIAM J. Numer. Anal. **44**(1) (2006) 183–198.

[34] S.-Y. Yi, *A Coupling of nonconforming and mixed finite element methods for Biot's consolidation model*. Numer. Methods Part. Diff. Eqns. **29**(5) (2013) 1749–1777.

[35] S.-Y. Yi, *Convergence analysis of a new mixed finite element method for Biot's consolidation model*. Numer. Methods Part. Diff. Eqns. **30** (2014) 1189–1210.

Centro de Investigación en Ingeniería Matemática (CI^{2}MA)

PRE-PUBLICACIONES 2018

2018-21 Ricardo Oyarzúa, Miguel Serón: *A divergence-conforming DG-mixed finite element method for the stationary Boussinesq problem*

2018-22 Veronica Anaya, Afaf Bouharguane, David Mora, Carlos Reales, Ricardo Ruiz-Baier, Nour Seloula, Hector Torres: *Analysis and approximation of a vorticity-velocity-pressure formulation for the Oseen equations*

2018-23 Ana Alonso-Rodriguez, Jessika Camaño, Eduardo De Los Santos, Francesca Rapetti: *A graph approach for the construction of high order divergence-free Raviart-Thomas finite elements*

2018-24 Raimund Bürger, Paul E. Méndez, Carlos Parés: *On entropy stable schemes for degenerate parabolic multispecies kinematic flow models*

2018-25 Jessika Camaño, Carlos Garcia, Ricardo Oyarzúa: *Analysis of a conservative mixed-FEM for the stationary Navier-Stokes problem*

2018-26 Mario Álvarez, Bryan Gomez-Vargas, Ricardo Ruiz-Baier, James Woodfield: *Stability and finite element approximation of phase change models for natural convection in porous media*

2018-27 Ricardo Oyarzúa, Manuel Solano, Paulo Zuñiga: *A high order mixed-FEM for diffusion problems on curved domains*

2018-28 Gabriel Carcamo, Stephanie Caro, Fabián Flores-Bazán: *Extensions of the standard quadratic optimization problem: strong duality, optimality, hidden convexity and S-lemma*

2018-29 Javier A. Almonacid, Hugo S. Díaz, Gabriel N. Gatica, Antonio Marquez: *A fully-mixed finite element method for the coupling of the Stokes and Darcy-Forchheimer problems*

2018-30 Raimund Bürger, Paul E. Méndez, Ricardo Ruiz-Baier: *On H(div)-conforming methods for double-diffusion equations in porous media*

2018-31 Rodolfo Araya, Rodolfo Rodríguez, Pablo Venegas: *Numerical analysis of a time-domain elastoacoustic problem*

2018-32 Sarvesh Kumar, Ricardo Oyarzúa, Ricardo Ruiz-Baier, Ruchi Sandilya: *Conservative discontinuous finite volume and mixed schemes for a new four-field formulation in poroelasticity*

Para obtener copias de las Pre-Publicaciones, escribir o llamar a: Director, Centro de Investigación en Ingeniería Matemática, Universidad de Concepción, Casilla 160-C, Concepción, Chile, Tel.: 41-2661324, o bien, visitar la página web del centro: http://www.ci2ma.udec.cl







Centro de Investigación en
Ingeniería Matemática (CI²MA)
Universidad de Concepción

Casilla 160-C, Concepción, Chile
Tel.: 56-41-2661324/2661554/2661316
http://www.ci2ma.udec.cl